JOURNAL OF MULTIFUNCTIONAL MATERIALS & PHOTOSCIENCE
9(1), June 2018, pp. 1-32

A Review: A Combination of Mesoporous Graphene, Titanium Dioxide, and Silica Materials with Other Semiconductors as High Performance Photocatalyst

Dinh Cung Tien Nguyen, Chang Sung Lim and Won-Chun Oh*

Department of Advanced Materials Science & Engineering, Hanseo University, Seosan, Chungnam, Korea, 356-706

Abstract: The environmental pollution is considered as one of the important issues today. One of the simple and effective methods for solving the problem of water pollution from industrial wastewater is from the photodegradation process. In the photocatalyst field, nanoparticles are one of the most promising candidates for technological applications. By far, mesoporous graphene with three-dimensional architectures has garnered increased attention recently from the fields of environmental research, sensors and biology. Mesoporous titanium dioxide has played a much larger role in this scenario compared to other semiconductor photocatalysts due to its cost effectiveness, inert nature and photostability. Silicate mesoporous materials have received widespread interest because of their potential applications as supports for catalysis, separation, selective adsorption, novel functional materials, and use as hosts to confine guest molecules, due to their extremely high surface areas combined with large and uniform pore sizes. Over time a constant demand has developed for larger pores with well-defined pore structures. The structure, composition, and pore size of these materials can be tailored during synthesis by variation of the reactant stoichiometry, the nature of the surfactant molecule, the auxiliary chemicals, the reaction conditions, or by post synthesis functionalization techniques. This review focuses mainly on a concise overview of mesoporous materials together with their applications as photocatalysts.

Keywords*:* Mesoporous TiO_2, Mesoporous SiO_2, Mesoporous Graphene, Graphene based composite, Photocatalyst

1. Introduction

Porous carbon materials are of interest in many applications because of their high surface area and physicochemical properties. Conventional syntheses can only produce randomly porous materials, with little control over the pore-size distributions, let alone mesostructures. Recent breakthroughs in the preparation of other porous materials have resulted in the development of methods for the preparation of mesoporous carbon materials with extremely high surface areas and ordered mesostructures, with potential applications as catalysts, separation media, and advanced electronic materials in many scientific

* Corresponding author*: wc_oh@hanseo.ac.kr*

disciplines. Current syntheses can be categorized as either hard template or soft-template methods.

Due to their unique electrical and mechanical properties, carbon materials have been employed as efficient catalyst supports in fuel cells to reduce the loading of catalysts while still render better catalytic activity, durability, and conductivity [1-3]. Reduced graphene oxide, carbon nanotubes, and mesoporous carbons have all been used as supports for cobalt oxides to catalyze ORR with better performance [4-7]. Graphene, a single-atom-thick carbon nanosheet, possesses large specific area, strong mechanical strength, as well as high electroconductivity and corrosion-resistance. These properties make it a promising material as catalyst support. However, the lack of highly reactive edge sites in graphene and the tendency of stacking together are detrimental to the catalysts coating and reactants diffusion [8]. Functional groups on graphene (which is properly oxidized) could be beneficial for the nucleation and anchoring of nanocrystals on the sheets to achieve covalent attachments but may otherwise lower the electroconductivity and put a limit on the catalytic efficiency of the hybrid materials [9-11].

Titania is a naturally occurring oxide known as titanium dioxide or titanium(IV) oxide with a chemical formula of TiO_2. Titania is well-known as one of the members of the family of transition metal oxide and the electronic configuration for the titanium metal is denoted as [Ar] 4s2 3d2. The metal oxide is intensely studied worldwide due to its interesting electrochemical properties, low cost, chemical stability, non-toxicity, resistance to photo-induced reaction and also commonly used in a various industrial application [12-17]. For instance, it can be used in the formulation of sunscreen, plastic, paper, toothpaste, foodstuffs and also as a white pigment in paints. Generally, minerals of titania can be found in one of the three crystalline form: anatase (tetragonal), rutile (tetragonal) or brookite (orthorhombic) [18]. Early breakthrough discovery, titania can be found coming from diversity of environmentally occurring ores which comprise of ilmenite, rutile, anatase along with leucoxene, where they are mined from sediments all over the world. For the record, majority of titania pigment in industry can be manufactured from titanium mineral ores by the so-called chloride or sulfate process, either as anatase or rutile form. The main titanium white-colored (use with regard to coloration pigments) nanoparticles are typically between 200 and 300 nm in diameter, even though there is some agglomeration formed. Titania also widely used in catalytic reaction acting as a promoter, a transporter for metals and metal oxides, an additive, or as a catalyst [19-21].

Mesoporous silica materials have been developed for some applications in the health field [22]. These solids are used for the controlled release of bioactive molecules, as catalysts in the synthesis of essential nutrients, as sensors to detect unhealthy products etc., with many applications in food technologies. By combining mesoporous silica materials with food, we can create healthier products, the products that improve our quality of life. The development of mesoporous materials applied to food could result in protecting bioactive molecules during their passage though the digestive system. For this reason, the controlled release of bioactive molecules is a very interesting topic for the discipline of food

technology. The use of mesoporous silica supports as catalysts in the synthesis of nutrients and as sensors for the detection of unhealthy products.

The development of graphene-based composites provides an important milestone to improve the application performance of metal oxide nanomaterials in different fields such as energy harvesting, conversion and storage devices, photovoltaic devices, photocatalysis, etc., because the hybrids have versatile and tailor-made properties with performances superior to those of the individual oxide nanomaterials [23-27]. Considerable efforts of decorating graphene with metal oxides NPs have recently been reported. To date, various kinds of metal oxides have been synthesized and supported on graphene, which include TiO_2, ZnO, SnO_2, MnO_2, Co_3O_4, Fe_3O_4, Fe_2O_3, NiO, Cu_2O, etc. [28-30]. To this end, many excellent studies have been published on the anchoring of the photocatalyst particles onto supports that are readily removable. As a response, several workers have coated photocatalysts onto a variety of surfaces, such as glass, silica gel, metal, ceramics, polymer, thin films, fibres, zeolite, alumina clays, activated carbon, cellulose, reactor walls and others [31-37].

2. Mesoporous Graphene

2.1. Porous carbon materials and mesoporous graphene

Porous carbon materials are ubiquitous and indispensable in many modern-day scientific applications. They are used extensively as electrode materials for batteries, fuel cells, and supercapacitors, as sorbents for separation processes and gas storage, and as supports for many important catalytic processes. Their use in such diverse applications is directly related not only to their superior physical and chemical properties, such as electric conductivity, thermal conductivity, chemical stability, and low density, but also to their wide availability. Many advances have been made in carbon technology in recent years, both through continued improvement of existing fabrication methods and through the development and introduction of new synthetic techniques. Conventional porous carbon materials, such as activated carbon and carbon molecular sieves, are synthesized by pyrolysis and physical or chemical activation of organic precursors, such as coal, wood, fruit shell, or polymers, at elevated temperatures. These carbon materials normally have relatively broad pore-size distributions in both micropore and mesopore ranges [38-41].

Graphene with three-dimensional architectures has garnered increased attention recently from the fields of environmental research, sensors and biology [42-44]. Nanoporous graphene foams with controlled pore sizes at nanoscales were firstly prepared by Zhao *et al.* [45]. Such 3D structures not only prevent graphene sheets from restacking but also provide graphene materials with a high specific surface area, an interconnected conductive network and a specific microenviroment due to the combination of a porous structure with the excellent intrinsic properties of graphene [46, 47]. It is anticipated that nanoporous graphene as a loading matrix would enhance the activity of embedded electrocatalysts [48].

Porous graphene materials can be prepared through hard-template methods by assembling graphene oxide (GO) with pre-formed solid templates, such as metal oxide particles, polymer spheres and coagulated aqueous solutions (hydrogel and freeze drying) or by depositing graphene onto porous catalysts (typically Ni foams) [49-58]. Nevertheless, the hard-template method involves complicated, expensive, and time consuming multistep procedures, which is the major disadvantage. On contrary, the soft-template method, using supramolecular aggregates, such as micelles and emulsions as templates, requires much fewer synthetic steps and has been proven to be an efficient technique for the synthesis of nanoporous siliceous and amorphous carbon materials with well-defined pore structures [59-64]. However, so far, few examples have been reported to synthesize porous graphene materials by the soft-template approach. We recently developed emulsion-template approach for the preparation of porous graphene materials [65]. However, the pore size control capability of that emulsion-template method is not satisfactory.

Moreover, graphene an important form of carbon allotrope, is gaining prevalence because of the industrial scalability, low cost (solution processable) and ease of hybridizing with other materials. Other benefits include visible light absorption, light weight, high specific surface area and outstanding chemical/ electrical stability characteristics which are advantageous for catalysis applications. Due to its myriad of benefits, composites of two-dimensional (2D) assemblies of graphene sheets with metal oxide and metal nanostructures have been explored [66-69]. However, to meet the demands of catalysis requirements of possessing a high surface area, porous structure and superior electrical conductivity, it is desirable to assemble the composite into a 3D framework [70, 71]. Forming a 3D interconnected framework (hydrogel) forms (i) desirable pores which facilitate liquid/gas access and diffusion, (ii) superior charge generation and collection of interconnected electrical pathways and (iii) conceptually ideal open structure for integration with other functional nanomaterials. Moreover, the size reduction of a photocatalyst to the nanoscale is often carried out to increase the reactive surface area, which brings about the difficulty in recovery after the catalysis process [72].

2.2. Application of mesoporous graphene as photocatalysts

Industrial and agricultural developments worsen water pollution in the world [73]. The water pollution represents a serious environmental problem and a public health concern. The aqueous organic pollutant is the main reason for lake eutrophication [74]. Organic pollutant removal from wastewater or eutrophic water has been a big challenge over the last decades, and up to date there is no single and economically attractive treatment that can effectively remove aqueous organic pollutant. Photocatalytic oxidation technology is an effective way of solving the problem of water pollution. Among photocatalysts, TiO_2 is most widely used because it is easily available, inexpensive, non-toxic, and has relatively high chemical stability [75]. However, as a wide band gap semiconductor (3.2 eV), TiO_2 can only absorb a UV fraction of solar light (3%–5%), which causes very low efficiency in solar light-assisted TiO_2 photocatalytic process performance [76]. On the other hand, the quantum efficiency of TiO_2 is low because of the fast recombination of photoinduced

electron–hole (e^-–h^+) pairs [77, 78]. To overcome these two drawbacks, many studies focused on designing novel TiO_2-based photocatalysts with high quantum efficiency and extending the light-response range through methods such as noble metal deposition, non-metal doping, and semiconductor coupling [79].

Kexin Li *et al.* [79] presented a mesoporous graphene and tourmaline co-doped titania composite was prepared using a direct sol–gel co-condensation combined with solvothermal treatment technique. The composite exhibited a three-dimensional (3D) interconnected mesostructure and anatase phase structure with a large surface area (218 m^2g^{-1}) and uniform pore size. Compared with pure titania, the photocatalytic activity of the composite was enhanced significantly towards aqueous organic pollutant rhodamine B and norfloxacin degradation under simulated sunlight irradiation. The high photocatalytic activities can be attributed to the enhanced quantum efficiency, narrowed band gap, and perfect surface physical and chemical properties of the composites. As efficient photocatalysts, the composites in the current study are expected to use solar light directly in wastewater treatment engineering (Fig. 1).

On the other hand, Minmin Gao et al [80] have developed a nanocomposite graphene hydrogel (NGH) based on green chemistry, employing vitamin C (VC) to attain a supramolecular 3D network of hybrid nanostructured materials. Here, it is shown that the hydrogel is an appropriate and robust host for stable a TiO_2 semiconductor catalyst sensitized with visible light responsive nanostructured particles. The NGH is tailored with well-defined nano-mesopores, a large surface area, a highly dispersive nanosheet–nanorods–nanoparticle composite, and enhance visible light absorption. Finally, we demonstrate practical applications of utilizing the NGH with water containing pores for

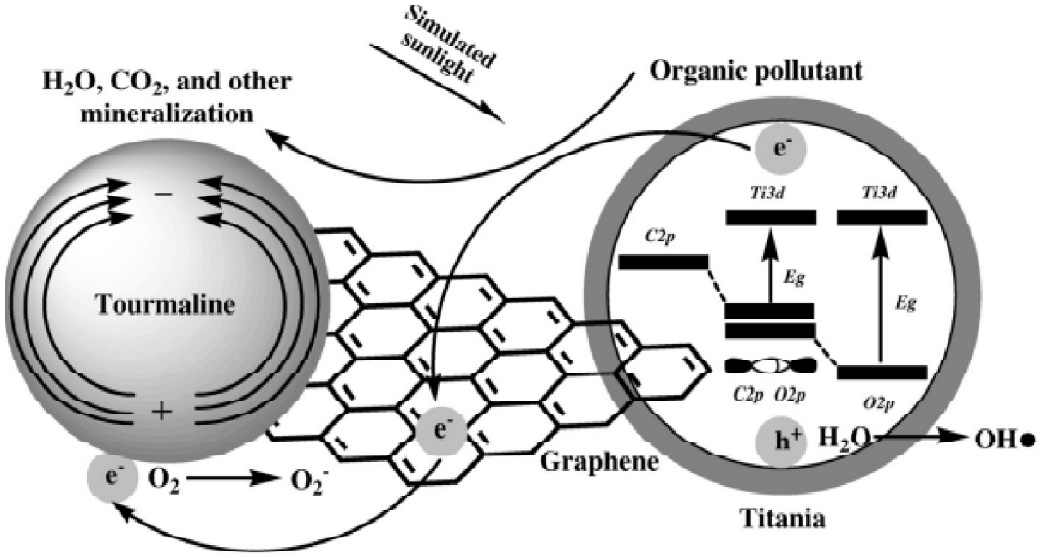

Figure 1: The transport and capture of photogenerated electrons in the graphene and tourmaline co-doped titania three component system, Ref. 79, Copyright (2002)).

photocatalytic H_2 production. An important pragmatic consideration of using an NGH is the ease of separation and recovery of the nanosized catalyst after the photoreaction which would otherwise require extensive and expensive nanofiltration (Fig. 2).

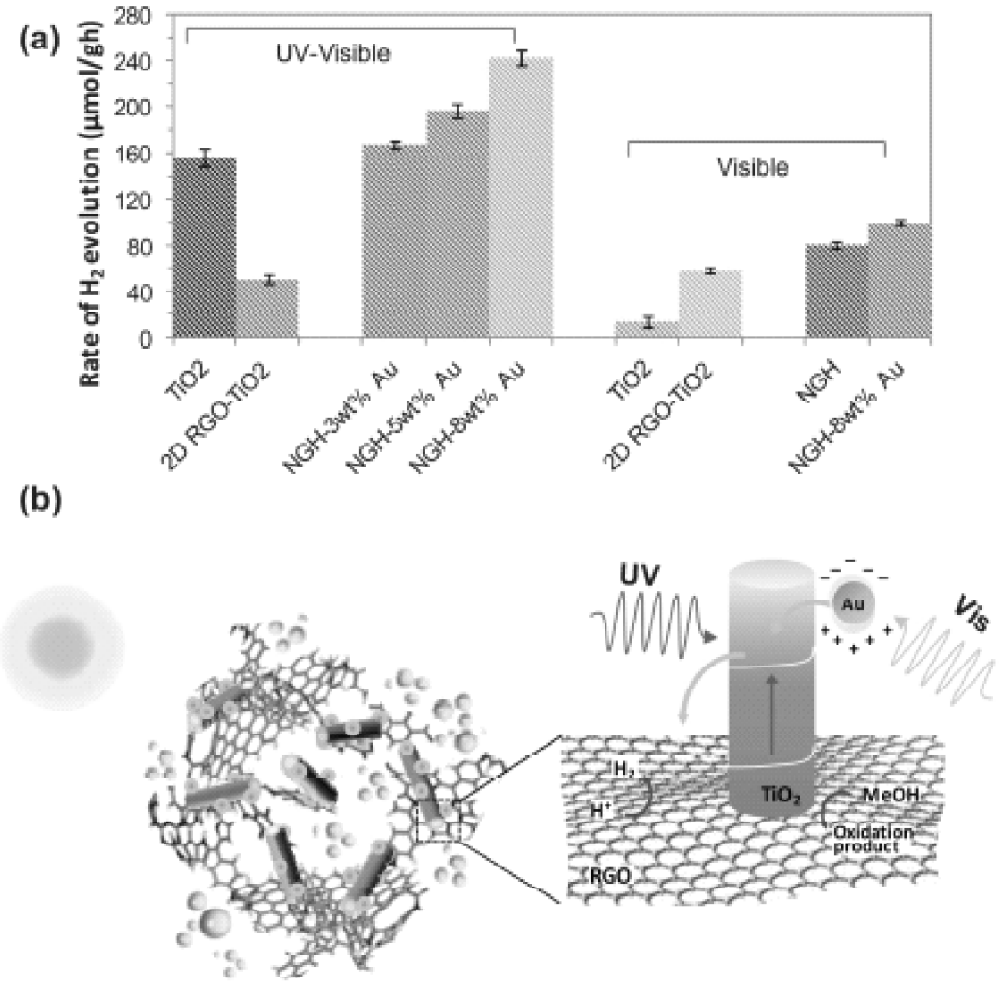

Figure 2: Photocatalytic H_2 production studies of the various samples. (a) H_2 production of the control samples (pure TiO_2 nanorods and 2D RGO–TiO_2 composite) and NGH with different wt% loading of Au nanoparticles under different light wavelength irradiations. (b) Proposed photocatalytic mechanism of the NGH–Au under ultraviolet and visible light irradiation, Ref. 80, Copyright (2002)).

Simulated sunlight photodegradation of aqueous atrazine and rhodamine B catalyzed by the ordered mesoporous graphene–titania/silica composite material was preserented by Kexin Li group [81]. Ordered mesoporous graphene–titania/silica composite material was prepared using a direct sol–gel co-condensation technique, and combined with hydrothermal treatment, in the presence of a triblock copolymer non-ionic surfactant P123

($EO_{20}PO_{70}EO_{20}$, EO=\$OCH_2CH_2$\, PO=\$OCH(CH_3)CH_2$\). The composite exhibited a two-dimensional (2D) hexagonal p6mm symmetry and anatase-phase structure with a large BET (Brunauer–Emmet–Teller) surface area and uniform pore size. The photocatalytic activity of the graphene–titania/silica composite was evaluated through the degradation of the aqueous organic pollutant atrazine and rhodamine B under solar-simulating Xe lamp irradiation. Enhanced photocatalytic activity compared with pure titania was obtained for the graphene titania/silica sample. In this study, at room temperature, P123 was dissolved into an HCl solution and tetraethyl orthosilicate (TEOS) was diluted with EtOH. A titanium tetrachloride/titanium tetraisopropoxide ($TiCl_4$/TTIP) solution was prepared by dropping $TiCl_4$ and TTIP into EtOH under vigorous stirring for 5 min. Graphene was dispersed equably in an EtOH/H_2O solution using an ultrasonic crasher for 1h. The above mentioned TEOS/EtOH, $TiCl_4$/TTIP/EtOH, and graphene/EtOH solutions were successively added dropwise into the P123/HCl solution. After stirring the resulting mixture for 24 h at room temperature, a semi-transparent sol was obtained. The sol was subjected to hydrothermal treatment at 150 °C for 48 h. The resulting gray hydrogel was dehydrated slowly at different temperature and reaction time, until a complete gel particulate was formed. After thermal treatment at 100°C for 24 h, the obtained powder was extracted using EtOH at 80 °C for 36 h to remove P123. Ordered mesoporous graphene–titania/silica composite material with unique physicochemical properties was obtained by carefully designing the preparation route. The composite material exhibited excellent photocatalytic activity in the degradation of aqueous organic pollutant atrazine and rhodamine B under solar simulating Xe lamp irradiation resulting from the enhanced quantum efficiency, ordered mesoporous structure, and perfect surface textural properties of the composite material. As an efficient photocatalyst, the threecomponent junction system composite material in this work is expected for use in the treatment of actual organic waste water.

Yuhan Li et al [82] reported an enhancing the photocatalytic activity of bulk g-C_3N_4 by introducing mesoporous structure and hybridizing with graphene. Graphitic carbon nitride (g-C_3N_4), can be used as an attractive metal-free organic photocatalyst that can work in visible light [83]. g-C_3N_4 possesses a high thermal and chemical stability as well as appealing electronic and optical properties. As a multifunctional catalyst, g-C_3N_4 has been applied in photosynthesis, energy conversion and storage, contaminants degradation carbon dioxide storage and reduction, solar cells, and sensing [84, 85]. Nevertheless, the photocatalytic efficiency of bulk g-C_3N_4 is limited because of its low surface area and the fast recombination rate of photogenerated electron–hole pairs. To resolve these problems, numerous strategies have been employed to modify the bulk g-C_3N_4, such as texture tuning by templates, band gap modification by heteroatoms doping, post-functionalization, and semiconductor coupling [86-92].

Bulk graphitic carbon nitride (CN) suffers from small surface area and high recombination of charge carriers, which result in low photocatalytic activity. To enhance the activity of g-C_3N_4, the surface area should be enlarged, and charge carrier separation should be promoted. In this work, a combined strategy was employed to dramatically

enhance the activity of bulk g-C_3N_4 by simultaneously introducing mesoporous structure and hybridizing with graphene/graphene oxide. The mesoporous g-C_3N_4/graphene (MCN-G) and mesoporous g-C_3N_4/graphene oxide (MCN-GO) nanocomposites with enhanced photocatalytic activity (NO removal ratio of 64.9% and 60.7%) were fabricated via a facile sonochemical method. The visible light harvesting ability of MCN-G and MCN-GO hybrids was enhanced and the conduction band was negatively shifted when 1.0 wt% graphene/graphene oxide was incorporated into the matrix of MCN. As electronic conductive channels, the G/GO sheets could efficiently facilitate the separation of charge carriers. MCN-G and MCN-GO exhibited drastically enhanced visible light photocatalytic activity toward NO removal. The NO removal ratio increased from 16.8% for CN to 64.9% for MCN-G and 60.7% for MCN-GO. This enhanced photocatalytic activity could be attributed to the increased surface area and pore volume, improved visible light utilization, enhanced reduction power of electrons, and promoted separation of charge carriers. This work demonstrates that a combined strategy is extremely effective for the development of active photocatalysts in environmental and energetic applications (Figs. 3-4). The enhanced activity of MCN-G and MCN-GO can be ascribed to the enlarged surface area and pore volume, increased light-harvesting ability, enhanced reduction power of photogenerated electrons, and improved charge carrier separation. This work shows that a combined strategy is effective for the modification of photocatalysts for large-scale applications.

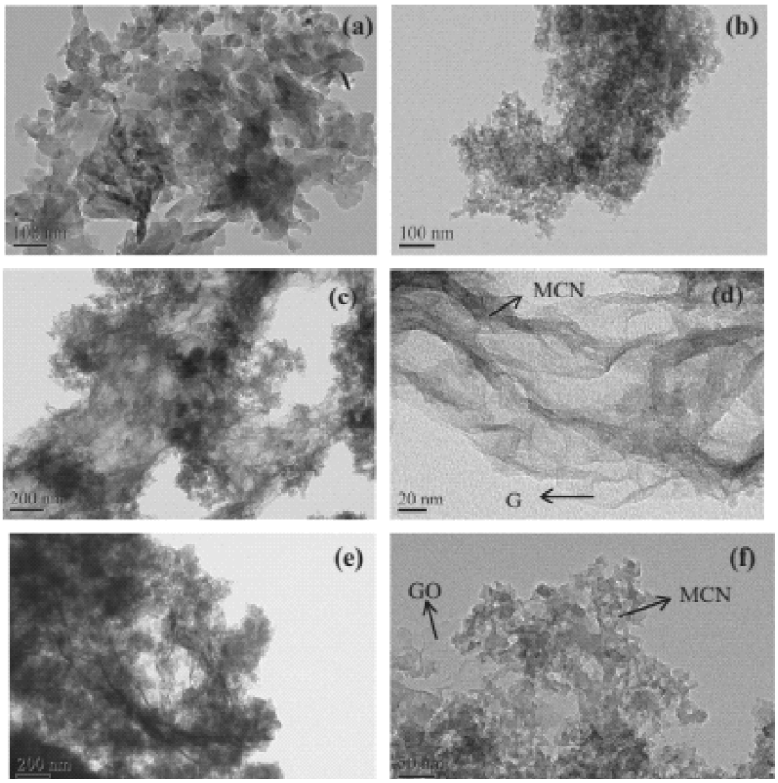

Figure 3: TEM images of CN (a), MCN (b), MCN-G (c, d), and MCN-GO (e, f), Ref. 82, Copyright (2014)).

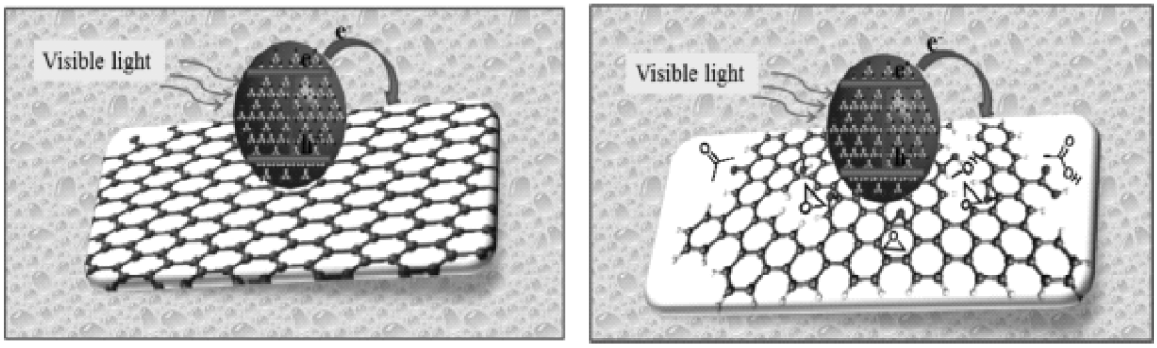

Figure 4: Schematic drawings of the photocatalytic induction process in the MCN-G (a) and MCN-GO (b) hybrids under visible light irradiation, Ref. 82, Copyright (2014)).

Lithium-ion batteries (LIBs) have become indispensable power source for cordless equipment (e.g. laptops) due to their outstanding advantages such as high energy density, long cycle life, no memory effect, environmental benignity, etc. Among these anode materials for LIBs, Sn and its compounds are very attractive because of their high theoretical specific capacity. Nevertheless, the practical use of Sn anodes is generally prevented by the severe volume change and the aggregation of Sn nanoparticles that occur during the alloying and dealloying process, resulting in rapid loss of capacity of the electrode and the end of the cycle life [93, 94]. Additionally, the particle size and structure of Sn may also influence its electrochemical properties [95]. To overcome the volume change and Sn particle aggregation, an alternative method is to disperse Sn nanoparticles in a protective carbon matrix such as bamboo-like hollow carbon nanofibers or spherical hollow carbon. These Sn–C composites delivered highly reversible and stable capacities after several cycles [96-98]. LIBs usually demonstrated better cycle performances and higher reversible capacities than bare Sn because graphene unit restrains the volume expansion and aggregation of Sn nanoparticles during the charge-discharge process [99-101]. the low Sn content in the graphene–Sn composite may reduce its theoretical capacity [102], while the high Sn content can induce the aggregation of Sn nanoparticles on the graphene surface, leading to the capacity loss and poor cycle performance. Wenbo Yue et al [103] presented a facile synthesis of mesoporous graphene-tin composites as high-performance anodes for lithium-ion batteries.

Graphene-based metals and their oxides usually exhibit enhanced electrochemical behavior in lithiumion batteries due to the outstanding properties of graphene. Moreover, the structure and morphology of electrodes can also take an important role in their electrochemical properties. Herein they describe a facile synthesis of graphene–Sn composites containing ca. 3–6 nm diameter mesopores formed by aggregation of Sn nanoparticles on the graphene surface. These mesoporous composites with large surface area deliver higher capacity and better cycle performance in comparison with pristine Sn particles. Furthermore, the mesoporous composites treated under hydrothermal treatment exhibit higher rechargeable capacities and cycle performances. In this study, graphene oxides were synthesized from natural graphite powders by a modified Hummer's method.

The mesoporous graphene–Sn composites were prepared by a facile one-step method. In brief, SnF_2. $2H_2O$ was added to GO suspension and then $NaBH_4$ aqueous solution was added dropwise into the above mixture solution with vigorous stirring. The upper solution was filtered, leaving the large Sn particles in the bottom. These graphene–Sn slurries were washed with distilled water repeatedly, dried at 40 °C. The graphene–Sn also synthesized using hydrothermal method. In brief, SnF_2 and $NaBH_4$ solution were added successively to GO suspension. The mixture solution was transferred into a Teflon-lined autoclave, sealed and heated in an oven at 90 °C for 6 h. The Sn content in the graphene-Sn composites was roughly analyzed by dispersing the composite in diluted hydrochloric acid. After dissolving Sn nanoparticles, the solid was dried. The solid containing graphene was weighed to evaluate the Sn content (Fig. 5). The mesoporous graphene–Sn composites exhibited much higher charge–discharge capacities than normal Sn particles due to their large surface areas and open pores. Moreover, increasing the surface area of mesoporous electrode may further accommodate more Li+ ion in the electrode, leading to a higher capacity. It is striking to note that bare Sn particles showed a significant capacity fading and poor cycle performance, whereas the mesoporous graphene–Sn composites exhibited better cycle performances. Their mesoporous structure may offer void volumes as buffer layers to protect the electrode from pulverization. Additionally, graphene coatings can also restrain the huge volume change and stabilize the mesostructured of graphene–Sn composites during cycles. It is worthwhile noting that G-Sn (1 h) and G–Sn (6 h) samples still suffered from visible capacity fading during cycles, which may result from the irremovable bare Sn particles. The efficient removal of bare Sn particles on the surface of mesoporous graphene–Sn composites will be explored in future. On the other hand, although the initial capacities were not as high as other graphene–Sn composites, the G–Sn(HM) sample delivered more stable reversible capacities. It can be attributed to the high crystallinity of graphene–Sn composites prepared under hydrothermal condition, which stabilized the crystal structure during the alloying and dealloying process. In conclusion, they developed a facile strategy to synthesize graphene–Sn composites with mesoporous structure as advanced anodes for LIBs. Sn nanoparticles with diameter under 5 nm were reduced by $NaBH_4$ solution and aggregated on the graphene surface to form

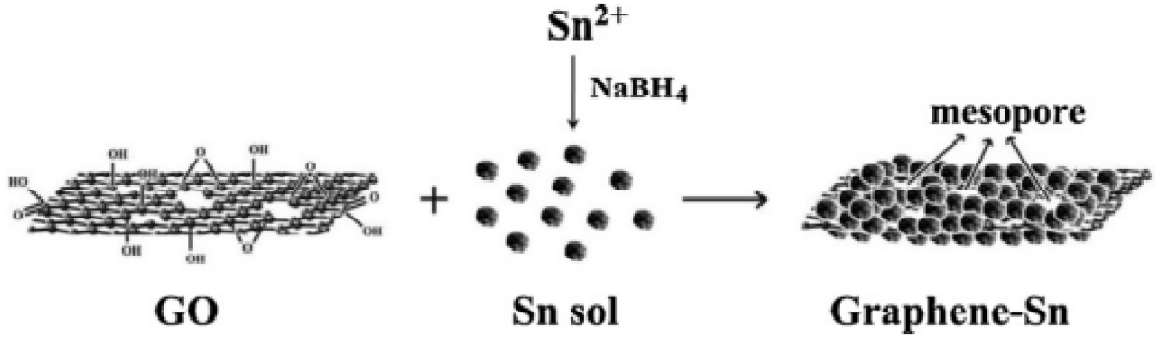

Figure 5: Schematic illustration of the synthetic route for mesoporous graphene–Sn, Ref. 103, Copyright (2013)).

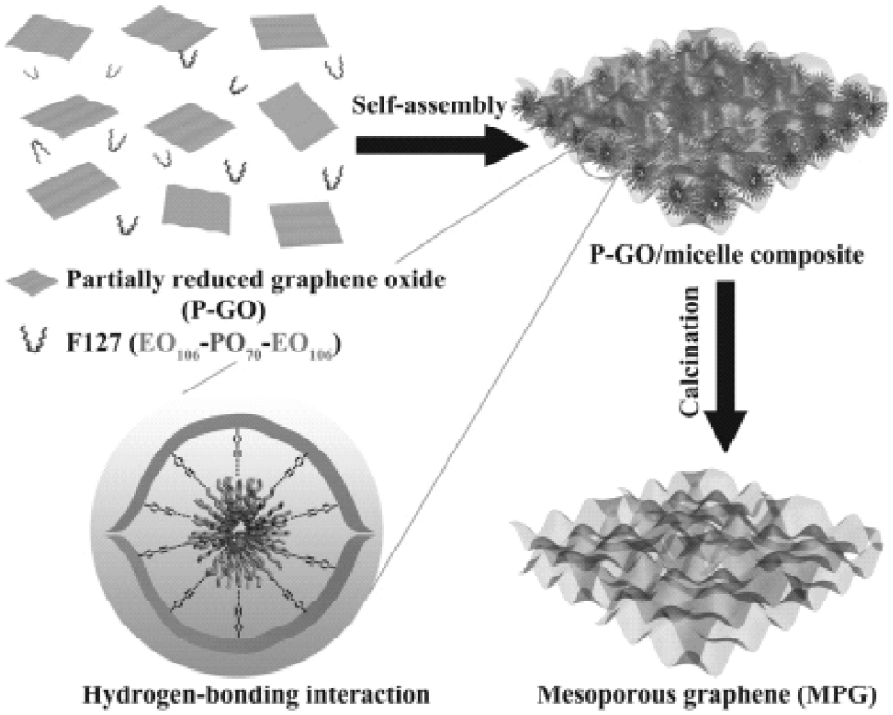

Figure 6: Schematic illustration for preparing mesoporous graphene. Self-assembly of partially reduced GO and F127 micelles, followed by calcination to obtain MPG, Ref. 104, Copyright (2014)).

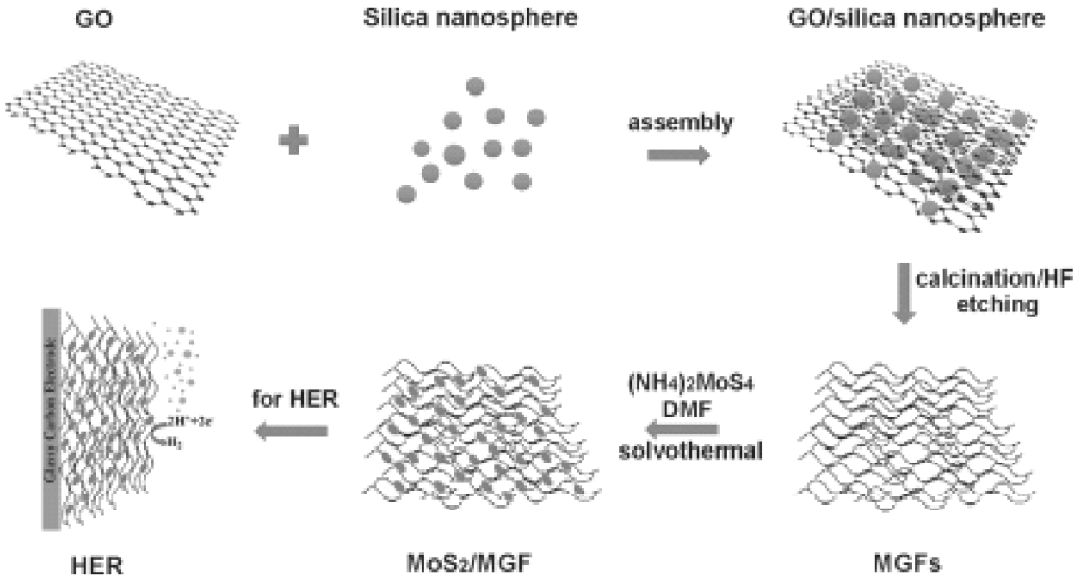

Figure 7: Illustration of the synthesis procedures of MoS_2/MGF using as an electrocatalyst for hydrogen evolution reaction, Ref. 113, Copyright (2013)).

the mesostructure. Mesoporous graphene–Sn composites exhibited enhanced electrochemical behaviors, especially after hydrothermal treatment. On one hand, their porous structure provided large surface areas and void volumes, which were beneficial to improve the electrode capacities and rate capabilities. On the other hand, the graphene substrate not only enhanced the electron conductivity, but also restrained the volume change and stabilized the mesostructure during the charge–discharge process. It can be expected that graphene-based materials with porous structure will be explored as catalysts, sensors or electrodes in future.

Hydrogen (H_2) is a promising secondary energy resource, with the advantages of high energy density and a carbon emission-free feature [104-106]. The electrochemical production of hydrogen from water splitting requires the use of catalysts, which can overcome the overpotential for the hydrogen evolution reaction (HER) and obtain high catalytic efficiency. Efficient electrocatalytic hydrogen evolutions using noble metals, metal alloys, enzymes, transition metal oxides and transition metal dichalcogenides catalysts have been extensively investigated [107-110]. Despite many progresses in pursuing new materials, most of the catalysts for HER contain metals, which are essential for the HER reaction, and they also require complicated preparation processes to expose sufficient catalytic active sites and increase electrical conductivities. An alternative approach for developing efficient and low-cost HER electrocatalysts is to synthesise carbon-based non-metal materials. Recently, heteroatoms doped graphene demonstrated potentials as metal-free electrocatalysts for hydrogen production46. The nitrogen (N) and phosphorus (P) heteroatoms could activate the adjacent carbon atoms in the graphene matrix by affecting their valence orbital energy levels to induce a synergistically enhanced reactivity toward HER [111].

Synthesis of mesoporous graphene materials by soft-template methods remains a great challenge, owing to the poor self-assembly capability of precursors and the severe agglomeration of graphene nanosheets. Herein, Xiaodan Huang *et al.* [112] presented a micelle-template strategy to prepare porous graphene materials with controllable mesopores, high specific surface areas and large pore volumes are reported. By fine-tuning the synthesis parameters, the pore sizes of mesoporous graphene can be rationally controlled. Nitrogen heteroatom doping is found to remarkably render electrocatalytic properties towards hydrogen evolution reactions as a highly efficient metal-free catalyst. The synthesis strategy and the demonstration of highly efficient catalytic effect provide benchmarks for preparing well-defined mesoporous graphene materials for energy production applications. In a typical synthesis process, GO aqueous suspension and hydrazine hydrate was mixed together at room temperature under vigorous stirring. After 12 h reaction, F127 aqueous solution (10 wt%) was introduced into the reaction suspension and subsequently stirred for 2 h. Then, HCl (37 wt%) was added. The entire system was reacted for a further 24 h under vigorous stirring at room temperature. The precipitate was collected by vacuum filtration. The obtained precipitate was firstly sintered at 350 ^{o}C in argon for 5 h and further heated at 900 ^{o}C for another 5 h under the argon atmosphere to obtain the final product, MPG. The porous architecture also contributes to the

significantly enhanced electrocatalytic efficiency. Moreover, porous graphene materials with relatively uniform mesopores have been successfully synthesized by a micelle-template method. The pore size and functionality of the mesoporous graphene materials can be well adjusted through tuning the synthesis parameters. By nitrogen-doping, the functionalized mesoporous graphene showed promising electrocatalytic performances for HER with high current densities and an excellent stability. Experimental investigations and theoretical stimulations demonstrated that the synergistic effect of mesoporous structure and nitrogen-functionalization could contribute to the significant enhancement of HER catalysis. The experimental results and fundamental understandings reported in this work provide a general protocol to design functional porous graphene materials and facilitate the development of new families of metal-free catalysts for hydrogen production.

Lei Liao *et al.* [113] presented MoS_2 formed on mesoporous graphene as a highly active catalyst for hydrogen evolution. A highly active and stable electrocatalyst for hydrogen evolution is developed based on the in-situ formation of MoS_2 nanoparticles on mesoporous graphene foams (MoS_2/MGF). Taking advantage of its high specific surface area and its interconnected conductive graphene skeleton, MGF provides a favorable microenvironment for the growth of highly dispersed MoS_2 nanoparticles while allowing rapid charge transfer kinetics. The MoS_2/MGF nanocomposites exhibit an excellent electrocatalytic activity for the hydrogen evolution reaction with a low overpotential and substantial apparent current densities. Such enhanced catalytic activity stems from the abundance of catalytic edge sites, the increase of electrochemically accessible surface area and the unique synergic effects between the MGF support and active catalyst. The electrode reactions are characterized by electrochemical impedance spectroscopy. A Tafel slope of H–42 mV per decade is measured for a MoS_2/MGF modified electrode, suggesting the Volmer-Heyrovsky mechanism of hydrogen evolution. These findings were attributed to an increased abundance of exposed catalytic edge sites and excellent electrical coupling to the underlying MGF modified electrode. MGF supported nano-MoS2 is a highly active electrocatalyst, making it a potential matrix for cost-effective catalysts in electrochemical hydrogen production.

3. Mesoporous Titanium Dioxide

3.1. A Perspective on Mesoporous TiO_2 Materials

Over the past two decades, various mesoporous materials with different compositions from pure inorganic or organic frameworks to organic-inorganic hybrid frameworks have been reported [114-117]. Among the families that experienced intensive advances, mesoporous TiO_2 is of particular interest and has been undergoing the most explosive growth due to its outstanding features such as low cost, environmental benignity, plentiful polymorphs, good chemical and thermal stability, excellent electronic and optical properties [118]. Compared with bulk TiO_2, uniform mesopore channels of the mesoporous TiO_2 do not only increase the density of active sites with high accessibility, but also facilitate the diffusion of reactants and products; the high surface area and large pore volume provide enhanced capability for dyes-loading and pollutants-adsorption. This has unambiguous

implications for photovoltaic, lithium-ion insertion and catalytic applications. Therefore, the design and synthesis of mesoporous TiO_2 with controllable mesopores and structures are important from both fundamental and technological viewpoints. Some excellent and exhaustive reviews have been published covering various aspects of mesoporous TiO_2, reflecting the tremendous advances in the past.

The sol-gel process of titanium precursors is distinguished from silicates by their higher chemical reactivity resulting from the lower electronegativity of titanium and its ability to exhibit several coordination states, so that coordination expansion occurs spontaneously upon reaction with water or even moisture [119]. Thus, titanium precursors tend to fast hydrolyze and form dense precipitates, which overwhelm the cooperative assembly with surfactants, leading to undesired phase separation. For example, the hydrolysis rate of titanium alkoxides is about 5 orders of magnitude faster than that of silicate ones. Therefore, the critical issue for preparing mesoporous TiO_2 under the guiding of surfactant templating is to control the hydrolysis and condensation rates of titanium precursors to effectively match the cooperative assembly with templates. In addition, the recovery of mesoporous TiO_2 without framework collapse should be paid much attention during the template removal and crystallization.

The use of preformed mesoporous solids as hard templates to synthesize mesoporous materials has brought in new possibilities for preparation of mesoporous TiO_2 with high crystallinity and novel mesostructure, which is well-known as hard-templating (nanocasting) method [120-121]. In this case, the mesopores arise from the regular arrangement of replicated nanowires/nanospheres via three key steps: (i) precursor infiltration inside mesochannels of the template; (ii) conversion of the precursor into target product in the mesochannels; (iii) removal of the mesoporous template. Obviously, compared with soft-templating method, the hard-templating method is less straightforward. However, this synthesis strategy not only avoids the control of the cooperative assembly and the sol–gel process of titanium precursors, but also easily overcomes the collapse of mesoporous TiO_2 frameworks during the phase transition process, thus making it quite successful and attractive on synthesis of ordered mesoporous TiO_2 with novel mesostructure, high thermal stability and crystallinity. However, it is not easy to completely fill up the vacancies of templates with titanium precursors because of their strong tendency to precipitate and crystallize into bulk oxide phases directly in aqueous media [122]. Some will partially block the channels, leading to failure in further infiltration.

3.2. Application of mesoporous graphene as photocatalysts

Dong Suk Kim *et al.* [123] presented the hydrothermal synthesis of mesoporous TiO_2 with high crystallinity, thermal stability, large surface area, and enhanced photocatalytic activity (Fig. 8). In this study, well-defined spherical mesoporous TiO_2 was prepared from a poly (ethylene glycol)-poly(propylene glycol) based triblock copolymer and titanium isopropoxide mixed with 2,4-pentanedione by using a simple sol–gel approach in aqueous solution. Hydrothermal treatment was performed to increase the crystallinity, thermal

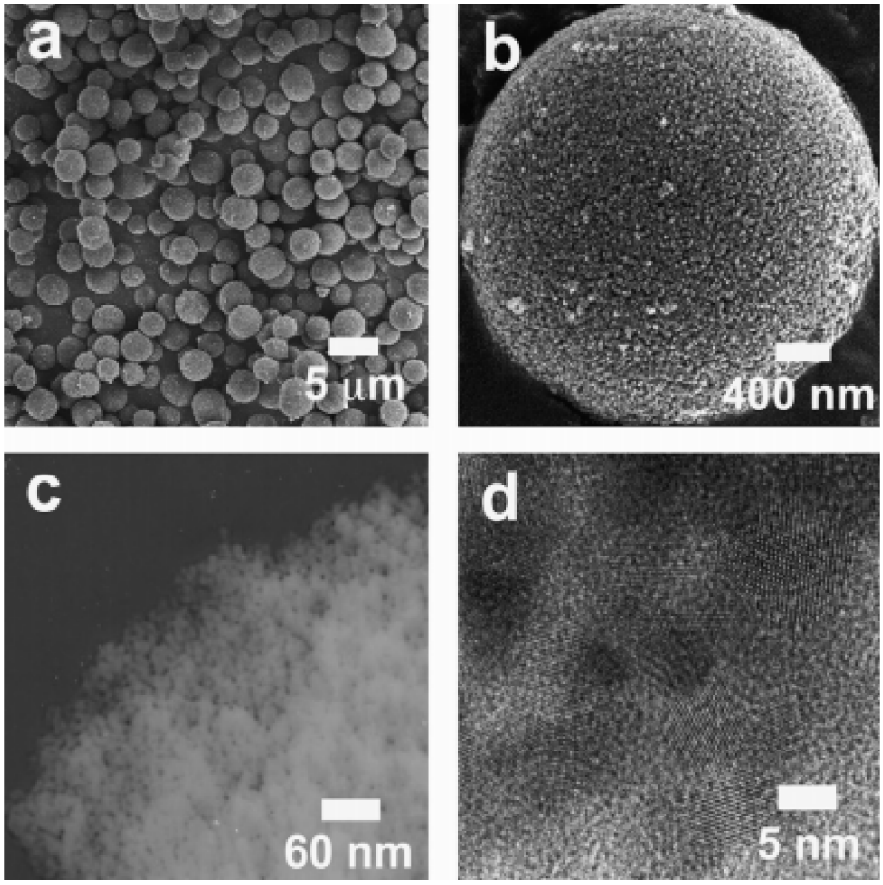

Figure 8: FE-SEM image of mesoporous TiO_2 with well-defined spherical shape (a), and magnified image of a selected area of one particle (b). TEM image of mesoporous TiO_2 (c), and magnified HR-TEM image of nanocrystalline anatase (d). Ref. 123, Copyright (2007)).

stability, surface area, and photocatalytic activity of the mesoporous TiO_2. The hydrothermally treated mesoporous TiO_2 materials were found to have a high crystallinity with a nanocrystalline anatase structure even in the as-synthesized state, whereas untreated materials were found to have an amorphous or semicrystalline phase prior to calcination at 300 °C. The surface area of hydrothermally treated mesoporous TiO_2 was found to exceed 395 m^2g^{-1}, whereas the areas of the untreated materials were less than 123 $m^2 g^{-1}$. The pore size distributions of the hydrothermally treated mesoporous TiO_2 materials were found to be narrower than those of untreated materials; the average pore size increased from 5.7 to 10.1 nm with increases in the calcination temperature. The photocatalytic activity of hydrothermally treated mesoporous TiO_2 is significantly higher than the activities of untreated materials, with a maximum decomposition rate that is three times faster than that of a commercial TiO_2, P25. The high photocatalytic activity of mesoporous TiO_2 is due to the large surface area and high crystallinity with a nanocrystalline anatase that is induced by the hydrothermal treatment. The high photocatalytic activity of the HTMT

materials in degradation of methylene blue can be explained in terms of their high crystallinities, large surface areas and small crystallite sizes. The use of aqueous solution as the reaction medium is environmentally friendly, and large amounts of materials can be synthesized with just one reaction at low cost. This method is expected to be applicable to the syntheses of other mesoporous transition metal oxides, and thus to be useful in many applications, such as photocatalysts, photovoltaics, and electronic sensors.

Comparative investigation on photocatalytic hydrogen evolution over Cu-, Pd-, and Au-loaded mesoporous TiO_2 photocatalysts was reported by Thammanoon Sreethawong group [124]. Photocatalytic activity for hydrogen evolution from water using methanol as hole scavenger was comparatively investigated over mesoporous TiO_2 photocatalysts with various contents of Cu, Pd, and Au cocatalyst loadings prepared by single-step sol–gel (SSSG) process with surfactant template. The comparison of optimum loading contents of the cocatalysts was chiefly studied on the mesoporous TiO_2. Among photocatalysts, 2 wt% Au supported on mesoporous TiO_2 exhibited the highest photocatalytic H_2 evolution activity. The Cu-, Pd-, and Au-loaded mesoporous TiO_2 photocatalysts with various loading contents were prepared by the single-step sol–gel process with surfactant template, in which the cocatalyst sources were introduced into the completely hydrolyzed TiO_2 sol prepared with templating surfactant acting as mesopore-directing agent. The photocatalytic performance of the loaded mesoporous TiO_2 samples was assessed by means of H_2 evolution from water using methanol as hole scavenger. The photocatalytic activity tests reveal that the optimum contents for Cu, Pd, and Au loadings were 1.5, 1, and 2 wt% at the H_2 evolution rate of 360, 420, and 557 lmol/h, respectively. At the optimum values, the H_2 evolution results show that the photocatalytic capability of the cocatalysts was in the order of Au > Pd > Cu. The 2 wt% Au-loaded mesoporous TiO_2 can be stated to be very active H_2 evolution photocatalyst in this comparative investigation.

Carbon nanotubes (CNTs) attract considerable attention since their discovery [125] due to their special structure, their extraordinary mechanical and unique electronic properties and their potential applications. Their high mechanical strength makes them to be good candidates for advanced composites [126]. They can either be semiconducting, semimetallic or metallic, depending on the helicity and the diameter of the tube [127]. Such variety opens a promising field in nanoscale electrodevice applications. Their large specific surface area, hollow and layered structures indicate that they can be ideal hydrogen storage materials [128]. Recently, researchers found that CNTs are efficient adsorbents for dioxin, fluoride, lead and cadmium [129]. Thus, CNTs can be used as a promising material in environmental cleaning. CNTs can conduct electrons [130] and have a high adsorption capacity. Anatase TiO_2 is known for its superior photocatalytic ability compared with other photocatalysts. Therefore, the application of CNTs to enhance the photocatalytic activity of TiO_2 is proposed. Ying Yu *et al.* [131] presented the enhancement of photocatalytic activity of mesoporous TiO_2 by using carbon nanotubes. Titanium dioxide/carbon nanotubes (TiO_2/CNTs) composites were prepared with the aid of ultrasonic irradiation. The photocatalytic activity was evaluated by the degradation of acetone and by the detection of the hydroxyl radical ($\cdot OH$) signals using electron paramagnetic resonance

(EPR). It is found that the crystalline TiO_2 is composed of both anatase and brookite phases. The agglomerated morphology and the particle size of TiO_2 in the composites change in the presence of CNTs. The CNTs in the composites are virtually all covered by TiO_2. Other than an increase of the surface area, the addition of CNTs does not affect the mesoporous nature of the TiO_2. Meanwhile, more hydroxyl groups are available on the surface of the composite than in the case of the pure TiO_2. The higher the content of CNTs, there is more effective in the suppression of the recombination of photo-generated e/h^+ pairs. However, excessive CNTs also shield the TiO_2 from absorbing UV light. The optimal amount of TiO_2 and CNTs is in the range of 1:0.1 and 1:0.2 (feedstock molar ratio). These samples have much more highly photocatalytic activity than P25 and TiO_2/activated carbon (AC) composite. The mechanism for the enhanced photocatalytic activity of TiO_2 by CNTs is proposed. The comparison of the photocatalytic activity of TiO_2 and TiO_2/CNTs composites for acetone degradation in air indicates that the presence of a small amount of CNTs can enhance photocatalytic activity of TiO_2 greatly. However, excess amount of CNTs also shield TiO_2 from absorbing UV. CNTs can enhance the photocatalytic activity of TiO_2 because the presence of CNTs can prevent the e/h+ pairs produced by TiO_2 under UV light from recombination. That is, electrons excited by TiO_2 may easily migrate to the nanostructure of the CNTs because of the strong interaction between TiO_2 and CNTs. Meanwhile, CNTs raise the band gap of TiO_2, which can make the e/h^+ pairs recombination less likely to occur. Moreover, the abundant hydroxyl groups adsorbed on the large surface of the composites can lead to the formation of more ·OH radicals. Therefore, through the two aspects, i.e. the decrease of the e/h^+ pairs recombination and more hydroxyl group on the surface of the composites, the photocatalytic activity of TiO_2 can be greatly enhanced by the presence of CNTs.

In view of the advantages the presence study attempted the synthesis of mesoporous Fe_2O_3/TiO_2 using P123 tri block copolymer by sol–gel method and examined the photocatalytic degradation of 4-chloropheenol, which is one of the important classes of water pollutant [132]. 4 -Chlorophenol is potentially a carcinogenic and mutagenic to mammalian as well as aquatic life. It is listed among the priority water pollutant by U.S.EPA [133]. It is generated as a by-product in plastic, paper making, insecticidal and petrochemical industries. It can cause serious effects on human health and environment [134]. Hence, design of a suitable process for complete mineralization of 4-chlorophenol in aqueous medium is an important issue. The photocatalytic degradation of 4-chlorophenol was extensively studied under UV-light illumination using MgAl hydrotalcites [135], mesoporous TiO_2 film [136] and Fe (III) citrate complex [137]. These materials showed promising photocatalytic efficiency in the degradation of 4-chlorophenol under UV-light irradiation. Photosensitization of TiO_2 with other transition metal oxides can extend its light absorption property in the visible region. Such materials could emerge as excellent catalysts for solar photocatalytic degradation. In the present study mesoporous Fe_2O_3/TiO_2 (10, 30, 50, 70 and 90 wt% Fe_2O_3) photocatalysts were synthesized by sol–gel process and characterized using different techniques. The XRD patterns exhibited the presence of mesoporous structure and isomorphic substitution of Fe^{3+} in TiO_2 at low Fe^{3+} loading and Ti^{4+} in Fe_2O_3 at high Fe^{3+} loading. The XPS results revealed the presence of

Ti^{4+} and Fe^{3+} in Fe_2O_3/TiO_2 materials. The DRS UV–vis spectra showed a shift in the band gap excitation of TiO_2 to longer wavelength, thus illustrating incorporation of Fe^{3+} in TiO_2. In addition, free TiO_2 and Fe_2O_3 particles were also present. Their photocatalytic activity was tested for the degradation of 4-chlorophenol in aqueous medium using sunlight. The activity of the catalysts followed the order: meso-30 wt% Fe_2O_3/TiO_2 > meso-10 wt% Fe_2O_3/TiO_2 > meso-50 wt% Fe_2O_3/TiO_2 > meso-70 Fe_2O_3/TiO_2 > meso-90 wt% Fe_2O_3/TiO_2 > meso-Fe_2O_3/TiO_2. This order concluded that mesoporous Fe_2O_3/TiO_2 could be an active catalyst for pollutant degradation, as TiO_2 with framework Fe^{3+} and photosensitization with free Fe_2O_3 were involved in the activity.

Minghua Zhou *et al.* [138] represented an effects of Fe doping on the photocatalytic activity of mesoporous TiO_2 powders prepared by an ultrasonic method. Highly photoactive nanocrystalline mesoporous Fe doped TiO_2 powders were prepared by the ultrasonic induced hydrolysis reaction of tetrabutyl titanate ($Ti(OC_4H_9)_4$) in a ferric nitrate aqueous solution (pH 5) without using any templates or surfactants. The photocatalytic activities were evaluated by the photocatalytic oxidation of acetone in air. The results showed that all the Fe-doped TiO_2 samples prepared by ultrasonic methods were mesoporous nanocrystalline. A small amount of Fe^{3+} ions in TiO_2 powders could obviously enhance their photocatalytic activity. The photocatalytic activity of Fe-doped TiO_2 powders prepared by this method and calcined at 400 ^oC exceeded that of Degussa P25 (P25) by a factor of more than two times at an optimal atomic ratio of Fe to Ti of 0.25. The high activities of the Fe-doped TiO_2 powders could be attributed to the results of the synergetic effects of Fe-doping, large BET specific surface area and small crystallite size.

4. Mesoporous Silica

4.1. Mesoporous silica nanoparticles

Mesoporous silica materials have attracted special attention after the discovery of a new family of molecular sieve called M41S. MCM-41, MCM-48, and SBA-15 are the most common mesoporous silica materials with the pore size ranging from 2 -10 nm and 2D-hexagonal and 3D-cubic structural characteristics [139]. The unique properties of mesoporous silica nanoparticles (MSNs) such as they have controlled particle size, porosity, morphology, and high chemical stability make nanoparticles highly attractive as drug carriers, diagnostic catalysis, separation and sensing [140-145]. Rapid internalization by animal and plant cells without causing any cytotoxicity inside the body, is another distinctive property of surface functionalized mesoporous silica nanoparticle [146, 147].

Mesoporous silica nanoparticles can be synthesized by using a surfactant in the aqueous solution which may be charged and neutral. Silicates (an ester of orthosilicic acid) are polymerized by surfactant [148]. The variables that involve controlling the size and morphology of mesoporous silica nanoparticles include:

- The rate of hydrolysis.
- The level of interaction between the assembled template and silica polymer.
- Condensation of silica source.

By controlling the pH, using different templates and co-solvent we control the above variables [149-151]. Stucky *et al.* synthesized hard mesoporous silica spheres having a size ranging from hundreds of microns up to millimeters at oil-water interphase, by using the high concentration of template and hydrophobic auxiliaries [152]. Stirring rate plays a key role in controlling the particle size of MSNs, if the rate is slow long fibers produced whereas upon fast stirring fine powder is formed [153]. The effect of pH on the morphology of MSNs was studied by Ozin *et al.* and demonstrates that under mild acidic condition spherical mesoporous particles with the range of 1-10 μm are formed [154]. Brinker *et al.* used a technique to synthesize MSNs ranging from 100-500 nm by evaporating solvent from aerosol containing silica source and surfactant [155].

4.2. Mesoporous silica application in the photocatalytic field

Ryuhei Nakamura *et al.* [156] reported a visible-light-driven water oxidation by Ir oxide clusters coupled to single Cr centers in mesoporous silica. Inert nanoporous oxides such as silica offer opportunities for assembling and coupling photocatalytic components for the direct conversion of water and carbon dioxide to fuel molecules under visible light. In these materials, framework substitution or covalent anchoring of metal centers and polynuclear components, and spatial separation of oxidizing from reducing sites can be explored by virtue of their surface chemistry and compartmentalized structure [157]. A particularly challenging task of this or any other approach to artificial photosynthesis is the visible light-driven oxidation of water. Of the small number of established oxygen-evolving catalysts, all are driven either electrochemically, by adding strong oxidants directly to the solution, or by generating the oxidant photochemically from a suitable precursor [158, 159]. To develop solar to fuel systems by integrating photocatalytic components into nanostructured scaffolds, direct coupling of the catalytic water oxidation site to a built-in visible light-driven electron pump is required [160]. Moreover, the chemical nature of the charge-transfer pump has to be such that it can be coupled to a reducing site in the nanoporous scaffold that accomplishes CO_2 or H^+ reduction. We report here an oxygen-evolving photocatalytic unit inside silica mesopores that consists of a single framework Cr (VI) center as a visible light absorbing electron pump coupled to an Ir oxide nanocluster. Visible-light-induced water oxidation has been demonstrated at a polynuclear catalyst coupled directly to a molecular charge-transfer moiety in a nanoporous solid. Covalently anchored metal centers as charge transfer chromophores open up opportunities for coupling the oxygen-evolving site to a reducing metal-to-metal charge-transfer unit in the nanoporous solid for accomplishing CO_2 reduction under H_2O oxidation in a sequential two-step process [161].

Yasutaka Kuwahara *et al.* [162] reported an efficient photocatalytic degradation of organics diluted in water and air using TiO_2 designed with zeolites and mesoporous silica materials. Titanium dioxide (TiO_2) is a promising photocatalyst for degradation of organic compounds ideally under environmentally benign conditions. This paper reviews recent developments in designing TiO_2-sorbent hybrid photocatalysts, especially those supported on ordered nano-porous silica materials including zeolites and mesoporous silicas, with

the objective of fabricating efficient photodegradation systems toward organic compounds diluted in water and air. This review also describes the basic features of zeolites and mesoporous silica, adsorption kinetics on their surfaces, and the principles of surface modification techniques, and highlights that the hydrophobic nature of support materials can offer significant enhancement in photodegradation. Contamination of water and air with harmful organic compounds, especially resulting from industries, still remains a major pollution problem, since they are often responsible for disruption of ecosystems as well as illness in the human body. Current environmental regulations require treatment and stabilization of these hazardous constituents and are anticipated to become more stringent in the future. To develop clean and safe chemical processes and materials contributing to this issue in accordance with the principles of green chemistry is our obligation, which should be undertaken with great urgency (Figs. 9-10).

Daisuke Tanaka *et al*. [163] reported an enhanced photocatalytic activity of quantum-confined tungsten trioxide nanoparticles in mesoporous silica. Due to quantum confinement effects, tungsten trioxide nanoparticles B1.4 nm in diameter prepared in channels of mesoporous silica exhibited a widened bandgap and enhanced photocatalytic performance in the decomposition of benzene. Tungsten trioxide (WO_3), employed in electrochromic devices [164], gas sensors [165], field emission devices [166], and photocatalysts [167], is an important semiconductor. Although the photocatalytic performance of WO_3 is weak due to minimal bandgap energy, reports indicate that it can be enhanced through platinum loading. However, improving the performance of WO_3 without using noble metals still remains a challenge. Recently, nanometric WO_3 has been

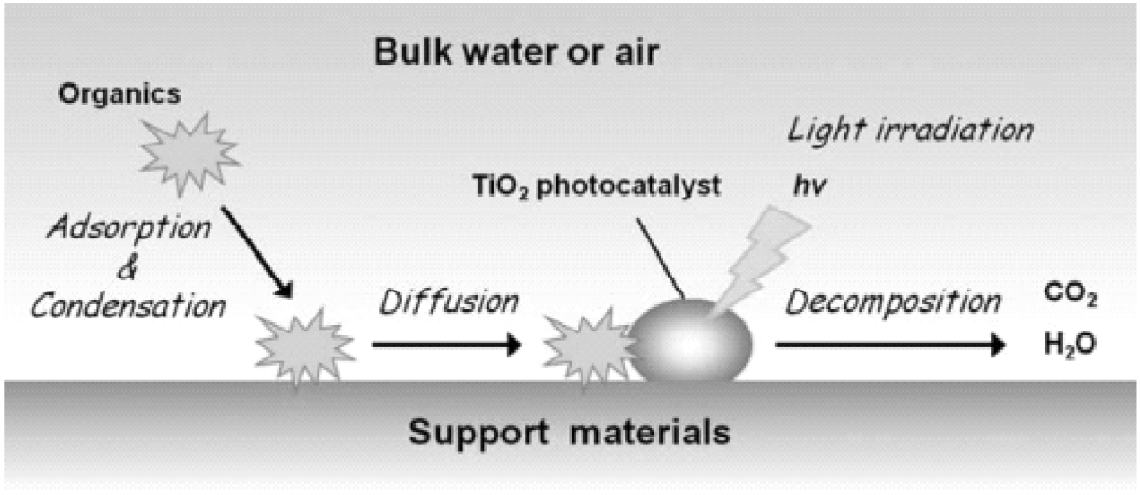

Figure 9: Adsorption and oxidation kinetics on the surface of supported TiO_2 photocatalyst. The organic substrates diluted in aqueous medium or atmosphere are considered to be first adsorbed on the surface of the support material where they migrate to the TiO_2 particles, and then are oxidized in the vicinity of TiO_2 by radical species such as hydroxyl radicals ($^{\cdot}OH$) and superoxide radical anions ($^{\cdot}O_2^-$) which are formed by the reaction with photogenerated holes (h^+) and electrons (e^-), respectively. Ref. 162, Copyright (2011)).

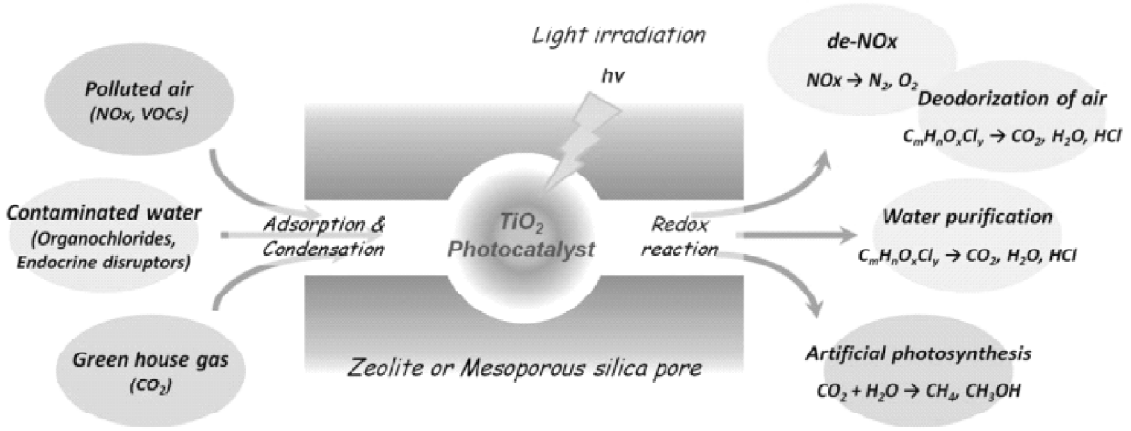

Figure 10: Applications of TiO_2 photocatalysts supported on nano-porous silicate materials in environmental protection, cleanup and energy conversion processes. Ref. 162, Copyright (2011)).

shown to possess many interesting properties arising from its specific structures. While several synthetic methods have been developed to obtain nanosized powders, WO_3 nanoparticles less than 2 nm in diameter have never been obtained, and this size is necessary to provide the quantum size effects [168-170]. Nevertheless, it is assumed that improved photocatalytic performance is possible through control and manipulation of the bandgap. Owing to the quantum size effect, nanometre-sized semiconductor particles are quite intriguing because of their fascinating optical and electronic properties. At the nanometre level, decreasing particle size widens the energy gap between the conduction and valence bands resulting in a blueshift at the absorption edge. The size-dependent optical properties of II–VI (chalcogenides) semiconductor nanocrystals, such as CdS and ZnO, have been well investigated for a wide variety of applications in optoelectronic devices and biological labelling [171-174].

In general, due to relatively minimal bandgap energy, aromatic compounds are not photocatalytically decomposed with bulk crystal of WO_3 [175]. Thus, the complete decomposition of toluene cannot be achieved with bulk WO_3. In the present study, however, using the 1.4-nm-size WO_3 particles for the photocatalytic decomposition of benzene was a success. While the photophysical properties of nanosized transition metal oxides displaying the quantum-size effect have been investigated, the quantum-size effects on catalytic performance have not sufficiently studied. Here, the photocatalytic activity of the WO_3 nanoparticles was evaluated using the decomposition of benzene under UV irradiation. Using a gas-chromatograph (Shimadzu, GC-8A), increments of CO_2 were measured from the decomposition of 200 ppm benzene vaporised in a glass bottle containing a 0.05 g sample. The decomposed benzene under UV irradiation from a black light (Toshiba, 6 W) was found with the micron-size WO_3. An initial increase in the amount of CO_2 is attributed to the decomposition of benzene by trapping photogenerated electrons via the reduction of W^{6+} to W^{5+} on the surface of WO_3 [176]. Since the electron capacity of WO_3 is limited, photodecomposition gradually decreases as the reaction progresses. In

the present study, the rate of CO_2 generation on micron-size WO_3 was relatively small and exhibited a saturating tendency. Fundamentally, the activation of oxygen molecules for the continuous oxidation of organics to CO_2 and H_2O is not induced on WO_3 due to its positive conduction band level [177]. Increments with the 1.8-nm size WO_3 particles in C16-MPS were vanishingly small because the amount of WO_3 was lower than that of the bulk WO_3 sample. On the other hand, after 28 h of irradiation, nearly all benzene was decomposed using the 1.4-nm-size WO_3 particles in C10-MPS. The vapor phase molecules were reacted with the nanosized WO_3 because the nanochannels in the silica were not completely occluded. This fact suggests that decreasing the size to a value below 1.5 nm enhances photocatalytic activity. It was reported that the decomposition of benzene was achieved with TiO_2 anatase with a bandgap of 3.2 eV. In fact, benzene was completely decomposed in several hours with commercial anatase powder (Ishihara ST-01) under the same conditions. Therefore, the enhanced performance of WO_3 nanoparticles is attributable to the enhanced reducing potential, through widening the bandgap in excess of 3.0 eV via the quantum-confinement effect.

Chih-Hung Huang *el al.* [178] reported a characterization and application of Ti-containing mesoporous silica for dye removal with the synergistic effect of coupled adsorption and photocatalytic oxidation. Highly ordered mesoporous silica, Santa Barbara Amorphous-15 (SBA-15), and titanium-substituted mesoporous silica (TiSBA-15) materials were successfully synthesized, characterized, and evaluated. A limited content of titanium could be effectively substituted into the framework of SBA-15 without provoking structure change. The adsorptive performance was examined by methylene blue (MB) adsorbed on prepared materials. The isotherm models were analyzed to describe the adsorption behavior of prepared materials. The adsorption isotherms were well fitted with Langmuir and Freundlich models in the simulation of the adsorption behavior of dyes. The SBA-15 and TiSBA-15 materials were found to be effective adsorbents for MB from aqueous solutions. The photodegradation of MB and total organic carbon (TOC) analysis on solid composites were used to evaluate the catalytical performance of Ti-containing mesoporous silica. The synergistic effect of adsorptive and photocatalytical ability of prepared TiSBA-15 was identified. The regeneration and cyclic performance were also proved. In this study, SBA-15 and TiSBA-15 samples with different nSi/nTi ratios were synthesized with the following molar gel composition P123/HCl/H_2O/TEOS/TTIP. In a typical synthesis, pluronic P123 was dissolved in distilled water and stirred at 35 °C for 2 h. Thereafter, HCl was then added to the clear solution and stirred for another 1 h. TEOS and the required amount of desired Ti source were added dropwise to the acid solution under vigorous stirring at 35 °C for 20 h. The resultant mixture was transferred into a polypropylene bottle and aged at 80 °C for another 20 h without stirring. The aged mixtures were filtered, washed, and dried at 100 °C overnight. After calcination at 500 °C for 5 h in air, the mesoporous products were obtained. Anatase TiO_2 has been formed and located on the external surface of SBA-15 with nSi/nTi value below 3. The analysis of adsorption behavior shows that the SBA-15 and TiSBA-15 are effective adsorbents for MB removal from aqueous solutions due to their high adsorption capacity. The adsorption isotherms can be well fitted with Langmuir and Freundlich models. The sorption capacity of MB follows the

order of SBA-15 > TiSBA-15[A] > TiSBA-15[B] > TiSBA-15 [C] > TiSBA-15[D]. The higher adsorption capacity of SBA-15 than that of TiSBA-15 is due to the effect of electrostatic attraction which is benefit to the adsorption intensity. The photodegradation of MB depends on the Ti content in the TiSBA-15 materials. However, TiSBA-15[A] and [B] exhibit better photodegradation rate normalized by per gram of Ti in synthesized samples. This photocatalytic behavior could be attributed to synergistic effect with adsorptive ability. After photocatalytic illumination, the structural regularity of TiSBA-15 is still maintained. TiSBA-15 exhibits advantages of adsorptive ability from mesoporous structure and photocatalytic performance by Ti incorporated into the framework. The organic molecules are largely adsorbed onto TiSBA-15 materials and then photo-degraded under UV irradiation. The process can be effectively recycled due to the regeneration capability of TiSBA-15. As a result, TiSBA-15 can be considered an ideal and effective material to remove organic pollutants in aqueous solution due to the synergetic effect of both adsorption and catalysis. Organic pollutants are supposed to be adsorbed or concentrated in situ and then degraded in vitro under factory process, while the mesoporous composites are regenerated and recycled.

5. Conclusions

The aim of this review has been to provide an overlook of the mesoporous silica, mesoporous graphene and mesoporous titania materials. Both these materials brought a good photocatalytic result. From that, we can hope that the problem of water pollution can be improved with the development of this material source. The high photodegradation performance is determined from a variety of different factors such as the graphene role, the reduced of the band gap energy values, the shape of the crystals of the achieved particles, so on. This catalyst can also be used to mineralize other organic pollutants in wastewater. Since the catalyst surface carried protons, amine-based pollutants such as dyes can be well adsorbed and decomposed rapidly. The increase of surface area can lead to the improvement of UV absorption and photoreactivity of photocatalysts. The photocatalytic performance of the loaded mesoporous TiO_2 samples was assessed by means of H_2 evolution from water using methanol as hole scavenger. The pore size and functionality of the mesoporous graphene materials can be well adjusted through tuning the synthesis parameters. The combination of the mesoporous adsorbents with hydrophobic surface and fine anatase TiO_2 photocatalyst is a good candidate as the efficient system for the degradation of organic pollutants diluted in water.

References

[1] Dinh Cung Tien Nguyen, Biswas Md Rokon Dowla, Yonrapach Areerob, et al. Copper Metallic Powder Effect for Expanded Graphite Plate for Thermal Conductivity, Asian Journal of Chemistry 29 (2017) 2154-2158.

[2] Dai, L., Chang, D. W., Baek, J. B., & Lu, W. (2012). Carbon nanomaterials for advanced energy conversion and storage. small, 8(8), 1130-1166.

[3] Dinh Cung Tien Nguyen, Dong-Hyen Oh and Won-Chun Oh, Immobilization of Bi_2O_3 Particles on Activated Carbon Fiber and Its Photodegradation Performance for Pollutant Dyes, Asian Journal of Chemistry 30 (2018) 491-498.

[4] Lee, D. U., Kim, B. J., & Chen, Z. (2013). One-pot synthesis of a mesoporous $NiCo_2O_4$ nanoplatelet and graphene hybrid and its oxygen reduction and evolution activities as an efficient bi-functional electrocatalyst. Journal of Materials Chemistry A, 1(15), 4754-4762.

[5] Liang, Y., Wang, H., Diao, P., Chang, W., Hong, G., Li, Y., ... & Regier, T. Z. (2012). Oxygen reduction electrocatalyst based on strongly coupled cobalt oxide nanocrystals and carbon nanotubes. Journal of the American Chemical Society, 134(38), 15849-15857.

[6] Liang, Y., Li, Y., Wang, H., Zhou, J., Wang, J., Regier, T., & Dai, H. (2011). Co_3O_4 nanocrystals on graphene as a synergistic catalyst for oxygen reduction reaction. Nature materials, 10(10), 780.

[7] Xu, J., Gao, P., & Zhao, T. S. (2012). Non-precious Co_3O_4 nano-rod electrocatalyst for oxygen reduction reaction in anion-exchange membrane fuel cells. Energy & Environmental Science, 5(1), 5333-5339.

[8] Yu, D., Wei, L., Jiang, W., Wang, H., Sun, B., Zhang, Q., ... & Chen, Y. (2013). Nitrogen doped holey graphene as an efficient metal-free multifunctional electrochemical catalyst for hydrazine oxidation and oxygen reduction. Nanoscale, 5(8), 3457-3464.

[9] Dinh Cung Tien Nguyen, Kwang-Youn Cho, Won-Chun Oh. Synthesis of mesoporous SiO_2/Cu_2O–graphene nanocomposites and their highly efficient photocatalytic performance for dye pollutants. RSC Adv. 7 (2017) 29284–29294.

[10] Liao, L., Zhu, J., Bian, X., Zhu, L., Scanlon, M. D., Girault, H. H., & Liu, B. (2013). MoS_2 formed on mesoporous graphene as a highly active catalyst for hydrogen evolution. *Advanced Functional Materials*, 23(42), 5326-5333.

[11] Dinh Cung Tien Nguyen and Won-Chun Oh. Ternary self-assembly method of mesoporous silica and Cu_2O combined graphene composite by nonionic surfactant and photocatalytic degradation of cationic-anionic dye pollutants. Separation and Purification Technology. 190 (2018) 77-89.

[12] Dinh Cung Tien Nguyen, Kwang-Youn Cho, Won-Chun Oh. New Synthesis of the Ternary Type Bi_2WO_6-GO-TiO_2 Nanocomposites by the Hydrothermal Method for the Improvement of the Photo-catalytic Effect. Appl. Chem. Eng. 28 (2017) 705-713.

[13] Bagheri, S., Mohd Hir, Z. A., Termeh Yousefi, A., & Abd Hamid, S. B. (2016). Photocatalytic performance of activated carbon-supported mesoporous titanium dioxide. Desalination and Water Treatment, 57(23), 10859-10865.

[14] Carp, O., Huisman, C. L., & Reller, A. (2004). Carbon-Inorganic hybrid materials: the carbon nanotube/ TiO_2 interface, Solid Prog. State Chem, 32, 42.

[15] Dinh Cung Tien Nguyen, Chang Sung Lim, and Won-Chun Oh, Mesoporous titanium dioxide and silica materials and its high application in photocatalytic performance: A review, Journal of Multifunctional Materials & Photoscience 8(2) 2017 163-197.

[16] Dinh Cung Tien Nguyen, Chang Sung Lim, and Won-Chun Oh, A self-assembly method to synthesis the binary/ternary type -graphene based composites and its high application in photocatalytic performance: A review, Journal of Multifunctional Materials & Photoscience 8(1) 2017 103-121.

[17] Bagheri, S., Hir, Z. A. M., Yousefi, A. T., & Hamid, S. B. A. (2015). Progress on mesoporous titanium dioxide: synthesis, modification and applications. Microporous and Mesoporous Materials, 218, 206-222.

[18] Ramimoghadam, D., Bagheri, S., & Abd Hamid, S. B. (2014). Biotemplated synthesis of anatase titanium dioxide nanoparticles via lignocellulosic waste material. BioMed research international, 2014.

[19] Muhd Julkapli, N., Bagheri, S., & Bee Abd Hamid, S. (2014). Recent advances in heterogeneous photocatalytic decolorization of synthetic dyes. The Scientific World Journal, 2014.

[20] Dinh Cung Tien Nguyen, Kwang-Youn Cho, Won-Chun Oh. A facile route to synthesize ternary Cu_2O quantum dot/graphene-TiO_2 nanocomposites with an improved photocatalytic effect. Fullerenes, Nanotubes and Carbon Nanostructures 27 (2017) 684-690.

[21] Dinh Cung Tien Nguyen, Kwang-Youn Cho, Won-Chun Oh. Synthesis of frost-like CuO combined graphene-TiO_2 by self-assembly method and its high photocatalytic performance. Applied Surface Science 412 (2017) 252–261.

[22] Bau, A. B., & Kourimská, L. (2013). Applications of mesoporous silica materials in food: a review. In Czech Journal of Food Sciences (Vol. 31, No. 2, pp. 99-107). Czech Academy of Agricultural Sciences.

[23] Kim KS, Zhao Y, Jang H, Lee SY, Kim JM, Kim KS, Ahn J-H, Kim P, Choi J-Y, Hong BH., Nature. 2009; 457:706.

[24] Pei SF, Cheng HM. The reduction of graphene oxide. Carbon. 2012; 50: 3210.

[25] Geng J, Kong BS, Yang SB, Jung HT. Chem Commun. 2010; 46:5091.

[26] Dinh Cung Tien Nguyen, Jung-Hun Woo, Kwang Youn Cho, Chong-Hun Jung, Won-Chun Oh. Highly efficient visible light driven photocatalytic activities of the $LaCuS_2$-graphene composite-decorated ordered mesoporous silica, Separation and Purification Technology 205 (2018) 11–21.

[27] Choucair M, Thordarson P, Stride JA. Nat Nanotechnol. 2009; 4:30.

[28] Bell NJ, Ng YH, Du AJ, Coster H, Smith SC, Amal R. J Phys Chem C. 2011; 115:6004.

[29] Huang XD, Zhou XF, Zhou L, Qian K, Wang YH, Liu ZP, Yu CZ. Chem Phys Chem. 2011; 12:278.

[30] Koo HY, Lee HJ, Go HA, Lee YB, Bae TS, Kim JK, Choi WS., Chem Eur J. 2011; 17:1214.

[31] J.H. Jean, T.A. Ring, Am. Ceram. Soc. Bull. 66 (12) (1986) 1574–1577.

[32] M.E. Fabiyi, R.L. Skelton, J. Photochem. Photobiol. A 129 (1999) 17–24.

[33] I. Turkevych, Y. Pihosh, M. Goto, A. Kasahara, M. Tosa, S. Kato, K. Takehana, T. Takamasu, G. Kido, N. Koguchi, Thin Solid Films 516 (2008) 2387–2391.

[34] M. Huang, C. Xu, Z. Wu, Y. Huang, J. Lin, J. Wu, Dyes Pigments 77 (2008) 327–334.

[35] R. Bellobono, I. Renato, A. Carrara, Effective Membrane Processes-New Perspectives, BHR, Mech. Engineer. Publ., London, 1993, pp. 257–274.

[36] V. Brezova, M. Jankovicova, M. Soldan, A. Blazkova, M. Rehakova, I. Surina, M. Ceppan, B. Havlinova, J. Photochem. Photobiol. A 83 (1994) 69–75.

[37] P. Monneyron, M.-H. Manero, J.-N. Foussard, F. Benoit-Marquié, M.-T. Maurette, Chem. Eng. Sci. 58 (2003) 971–978.

[38] R. C. Bansal, J. B. Donnet, F. Stoeckli, Active Carbon, Marcel Dekker, New York, 1988.

[39] R. T. Yang, Adsorbents: Fundamentals and Applications, WileyInterscience, New York, 2003.

[40] T. R. Gaffney, Curr. Opin. Solid State Mater. Sci. 1996, 1, 69.

[41] Liang, C., Li, Z., & Dai, S. (2008). Mesoporous carbon materials: synthesis and modification. Angewandte Chemie International Edition, 47(20), 3696-3717.

[42] Zhu, S., Tang, S., Zhang, J., & Yang, B. (2012). Control the size and surface chemistry of graphene for the rising fluorescent materials. Chemical communications, 48(38), 4527-4539.

[43] He, Q., Wu, S., Yin, Z., & Zhang, H. (2012). Graphene-based electronic sensors. Chemical Science, 3(6), 1764-1772.

[44] Chen, Q., Zhang, L., & Chen, G. (2011). Facile preparation of graphene-copper nanoparticle composite by in situ chemical reduction for electrochemical sensing of carbohydrates. Analytical chemistry, 84(1), 171-178.

[45] Huang, X., Qian, K., Yang, J., Zhang, J., Li, L., Yu, C., & Zhao, D. (2012). Functional nanoporous graphene foams with controlled pore sizes. Advanced Materials, 24(32), 4419-4423.

[46] Li, C., & Shi, G. (2012). Three-dimensional graphene architectures. Nanoscale, 4(18), 5549-5563.

[47] Dong, X. C., Xu, H., Wang, X. W., Huang, Y. X., Chan-Park, M. B., Zhang, H., ... & Chen, P. (2012). 3D graphene–cobalt oxide electrode for high-performance supercapacitor and enzymeless glucose detection. ACS nano, 6(4), 3206-3213.

[48] Liao, L., Zhu, J., Bian, X., Zhu, L., Scanlon, M. D., Girault, H. H., & Liu, B. (2013). MoS2 formed on mesoporous graphene as a highly active catalyst for hydrogen evolution. Advanced Functional Materials, 23(42), 5326-5333.

[49] Huang, X., Qian, K., Yang, J., Zhang, J., Li, L., Yu, C., & Zhao, D. (2012). Functional nanoporous graphene foams with controlled pore sizes. Advanced Materials, 24(32), 4419-4423.

[50] Yang, S., Feng, X., Ivanovici, S., & Müllen, K. (2010). Fabrication of graphene encapsulated oxide nanoparticles: towards high performance anode materials for lithium storage. Angewandte Chemie International Edition, 49(45), 8408-8411.

[51] Sohn, K., Na, Y. J., Chang, H., Roh, K. M., Jang, H. D., & Huang, J. (2012). Oil absorbing graphene capsules by capillary molding. Chemical Communications, 48(48), 5968-5970.

[52] Qiu, L., Liu, J. Z., Chang, S. L., Wu, Y., & Li, D. (2012). Biomimetic superelastic graphene-based cellular monoliths. Nature communications, 3, 1241.

[53] Wang, Z. L., Xu, D., Wang, H. G., Wu, Z., & Zhang, X. B. (2013). In situ fabrication of porous graphene electrodes for high-performance energy storage. ACS nano, 7(3), 2422-2430.

[54] Wu, Z. S., Sun, Y., Tan, Y. Z., Yang, S., Feng, X., & Mullen, K. (2012). Three-dimensional graphene-based macro-and mesoporous frameworks for high-performance electrochemical capacitive energy storage. Journal of the American Chemical Society, 134(48), 19532-19535.

[55] Zhao, Y., Hu, C., Hu, Y., Cheng, H., Shi, G., & Qu, L. (2012). A versatile, ultralight, nitrogen doped graphene framework. Angewandte chemie, 124(45), 11533-11537.

[56] Sun, H., Xu, Z., & Gao, C. (2013). Multifunctional, ultra flyweight, synergistically assembled carbon aerogels. Advanced Materials, 25(18), 2554-2560.

[57] Ito, Y. *et al*. High-quality three-dimensional nanoporous graphene. Angew. Chem. Int. Ed. 126, 4922–4926 (2014).

[58] Chen, Z., Ren, W., Gao, L., Liu, B., Pei, S., & Cheng, H. M. (2011). Three-dimensional flexible and conductive interconnected graphene networks grown by chemical vapour deposition. Nature materials, 10(6), 424.

[59] Wan, Y., & Zhao, D. (2007). On the controllable soft-templating approach to mesoporous silicates. Chemical reviews, 107(7), 2821-2860.

[60] Li, W., Yue, Q., Deng, Y., & Zhao, D. (2013). Ordered mesoporous materials based on interfacial assembly and engineering. Advanced Materials, 25(37), 5129-5152.

[61] Valtchev, V., & Tosheva, L. (2013). Porous nanosized particles: preparation, properties, and applications. Chemical reviews, 113(8), 6734-6760.

[62] Deng, Y., Wei, J., Sun, Z., & Zhao, D. (2013). Large-pore ordered mesoporous materials templated from non-Pluronic amphiphilic block copolymers. Chemical Society Reviews, 42(9), 4054-4070.

[63] Ma, T. Y., Liu, L., & Yuan, Z. Y. (2013). Direct synthesis of ordered mesoporous carbons. Chemical Society Reviews, 42(9), 3977-4003.

[64] Liu, J., Yang, T., Wang, D. W., Lu, G. Q. M., Zhao, D., & Qiao, S. Z. (2013). A facile soft-template synthesis of mesoporous polymeric and carbonaceous nanospheres. Nature communications, 4, 2798.

[65] Huang, X., Zhao, Y., Ao, Z., & Wang, G. (2014). Micelle-template synthesis of nitrogen-doped mesoporous graphene as an efficient metal-free electrocatalyst for hydrogen production. Scientific reports, 4, 7557.

[66] Zhang, X. Y., Li, H. P., Cui, X. L., & Lin, Y. (2010). Graphene/TiO_2 nanocomposites: synthesis, characterization and application in hydrogen evolution from water photocatalytic splitting. Journal of Materials Chemistry, 20(14), 2801-2806.

[67] Wong, T. J., Lim, F. J., Gao, M., Lee, G. H., & Ho, G. W. (2013). Photocatalytic H_2 production of composite one-dimensional TiO_2 nanostructures of different morphological structures and crystal phases with graphene. Catalysis Science & Technology, 3(4), 1086-1093.

[68] Xiang, Q., Yu, J., & Jaroniec, M. (2011). Enhanced photocatalytic H_2-production activity of graphene-modified titania nanosheets. Nanoscale, 3(9), 3670-3678.

[69] Zhang, H., Lv, X., Li, Y., Wang, Y., & Li, J. (2009). P25-graphene composite as a high performance photocatalyst. ACS nano, 4(1), 380-386.

[70] Cong, H. P., Ren, X. C., Wang, P., & Yu, S. H. ACS Nano, 2012, 6, 2693–2703. CrossRef| CAS| Web of Science® Times Cited, 114.

[71] Xu, Y., Sheng, K., Li, C., & Shi, G. (2010). Self-assembled graphene hydrogel via a one-step hydrothermal process. ACS nano, 4(7), 4324-4330.

[72] Gao, M., Peh, C. K. N., Ong, W. L., & Ho, G. W. (2013). Green chemistry synthesis of a nanocomposite graphene hydrogel with three-dimensional nano-mesopores for photocatalytic H_2 production. RSC Advances, 3(32), 13169-13177.

[73] Guo, C., Ge, M., Liu, L., Gao, G., Feng, Y., & Wang, Y. (2009). Directed synthesis of mesoporous microspheres: catalysts and their photocatalysis for bisphenol A degradation. Environmental science & technology, 44(1), 419-425.

[74] Chen, P., Zhu, L., Fang, S., Wang, C., & Shan, G. (2012). Photocatalytic degradation efficiency and mechanism of microcystin-RR by mesoporous Bi_2WO_6 under near ultraviolet light. Environmental science & technology, 46(4), 2345-2351.

[75] Xiang, Q., Yu, J., & Jaroniec, M. (2012). Synergetic effect of MoS_2 and graphene as cocatalysts for enhanced photocatalytic H_2 production activity of TiO_2 nanoparticles. Journal of the American Chemical Society, 134(15), 6575-6578.

[76] Li, K., Yang, X., Guo, Y., Ma, F., Li, H., Chen, L., & Guo, Y. (2010). Design of mesostructured $H_3PW_{12}O_{40}$–titania materials with controllable structural orderings and pore geometries and their simulated sunlight photocatalytic activity towards diethyl phthalate degradation. Applied Catalysis B: Environmental, 99(1-2), 364-375.

[77] Dutta, S., Patra, A. K., De, S., Bhaumik, A., & Saha, B. (2012). Self-assembled TiO_2 nanospheres by using a biopolymer as a template and its optoelectronic application. ACS applied materials & interfaces, 4(3), 1560-1564.

[78] Kundu, S., Vidal, A. B., Yang, F., Ramírez, P. J., Senanayake, S. D., Stacchiola, D., ... & Rodriguez, J. A. (2012). Special Chemical Properties of RuO_x Nanowires in RuO_x/TiO_2 (110): Dissociation of Water and Hydrogen Production. The Journal of Physical Chemistry C, 116(7), 4767-4773.

[79] Li, K., Chen, T., Yan, L., Dai, Y., Huang, Z., Guo, H., ... & Song, D. (2012). Synthesis of mesoporous graphene and tourmaline co-doped titania composites and their photocatalytic activity towards organic pollutant degradation and eutrophic water treatment. Catalysis Communications, 28, 196-201.

[80] Gao, M., Peh, C. K. N., Ong, W. L., & Ho, G. W. (2013). Green chemistry synthesis of a nanocomposite graphene hydrogel with three-dimensional nano-mesopores for photocatalytic H_2 production. RSC Advances, 3(32), 13169-13177.

[81] Li, K., Huang, Y., Yan, L., Dai, Y., Xue, K., Guo, H., ... & Xiong, J. (2012). Simulated sunlight photodegradation of aqueous atrazine and rhodamine B catalyzed by the ordered mesoporous graphene–titania/silica composite material. Catalysis Communications, 18, 16-20.

[82] Li, Y., Sun, Y., Dong, F., & Ho, W. K. (2014). Enhancing the photocatalytic activity of bulk g-C3N4 by introducing mesoporous structure and hybridizing with graphene. Journal of colloid and interface science, 436, 29-36.

[83] Wang, X., Maeda, K., Thomas, A., Takanabe, K., Xin, G., Carlsson, J. M., ... & Antonietti, M. (2009). A metal-free polymeric photocatalyst for hydrogen production from water under visible light. Nature materials, 8(1), 76.

[84] Wang, Y., Wang, X., & Antonietti, M. (2012). Polymeric graphitic carbon nitride as a heterogeneous organocatalyst: from photochemistry to multipurpose catalysis to sustainable chemistry. Angewandte Chemie International Edition, 51(1), 68-89.

[85] Zheng, Y., Liu, J., Liang, J., Jaroniec, M., & Qiao, S. Z. (2012). Graphitic carbon nitride materials: controllable synthesis and applications in fuel cells and photocatalysis. Energy & Environmental Science, 5(5), 6717-6731.

[86] Long, B., Ding, Z., & Wang, X. (2013). Carbon nitride for the selective oxidation of aromatic alcohols in water under visible light. ChemSusChem, 6(11), 2074-2078.

[87] Zhang, J., Guo, F., & Wang, X. (2013). An optimized and general synthetic strategy for fabrication of polymeric carbon nitride nanoarchitectures. Advanced Functional Materials, 23(23), 3008-3014.

[88] Jiang, D., Zhu, J., Chen, M., & Xie, J. (2014). Highly efficient heterojunction photocatalyst based on nanoporous g-C3N4 sheets modified by Ag_3PO_4 nanoparticles: Synthesis and enhanced photocatalytic activity. Journal of colloid and interface science, 417, 115-120.

[89] Lin, Z., & Wang, X. (2013). Nanostructure engineering and doping of conjugated carbon nitride semiconductors for hydrogen photosynthesis. Angewandte Chemie International Edition, 52(6), 1735-1738.

[90] Zhang, J., Zhang, M., Sun, R. Q., & Wang, X. (2012). A facile band alignment of polymeric carbon nitride semiconductors to construct isotype heterojunctions. Angewandte Chemie, 124(40), 10292-10296.

[91] Dong, F., Zhao, Z., Xiong, T., Ni, Z., Zhang, W., Sun, Y., & Ho, W. K. (2013). In situ construction of g-C3N4/g-C3N4 metal-free heterojunction for enhanced visible-light photocatalysis. ACS applied materials & interfaces, 5(21), 11392-11401.

[92] Dong, F., Li, Y., Ho, W., Zhang, H., Fu, M., & Wu, Z. (2014). Synthesis of mesoporous polymeric carbon nitride exhibiting enhanced and durable visible light photocatalytic performance. Chinese science bulletin, 59(7), 688-698.

[93] Winter, M., & Besenhard, J. O. (1999). Electrochemical lithiation of tin and tin-based intermetallics and composites. Electrochimica Acta, 45(1-2), 31-50.

[94] Nimisha, C. S., Venkatesh, G., Rao, K. Y., Rao, G. M., & Munichandraiah, N. (2012). Morphology dependent electrochemical performance of sputter deposited Sn thin films. Materials Research Bulletin, 47(8), 1950-1953.

[95] Whitehead, A. H., Elliott, J. M., & Owen, J. R. (1999). Nanostructured tin for use as a negative electrode material in Li-ion batteries. Journal of Power Sources, 81, 33-38.

[96] Hassoun, J., Derrien, G., Panero, S., & Scrosati, B. (2008). A nanostructured Sn–C composite lithium battery electrode with unique stability and high electrochemical performance. Advanced Materials, 20(16), 3169-3175.

[97] Yu, Y., Gu, L., Wang, C., Dhanabalan, A., Van Aken, P. A., & Maier, J. (2009). Encapsulation of Sn@ carbon nanoparticles in bamboo like hollow carbon nanofibers as an anode material in lithium based batteries. Angewandte Chemie International Edition, 48(35), 6485-6489.

[98] Wu, P., Du, N., Liu, J., Zhang, H., Yu, J., & Yang, D. (2011). Solvothermal synthesis of carbon-coated tin nanorods for superior reversible lithium ion storage. Materials Research Bulletin, 46(12), 2278-2282.

[99] Wang, G., Wang, B., Wang, X., Park, J., Dou, S., Ahn, H., & Kim, K. (2009). Sn/graphene nanocomposite with 3D architecture for enhanced reversible lithium storage in lithium ion batteries. Journal of Materials Chemistry, 19(44), 8378-8384.

[100] Ji, L., Tan, Z., Kuykendall, T., An, E. J., Fu, Y., Battaglia, V., & Zhang, Y. (2011). Multilayer nanoassembly of Sn-nanopillar arrays sandwiched between graphene layers for high-capacity lithium storage. Energy & Environmental Science, 4(9), 3611-3616.

[101] Gu, Y., Xu, Y., & Wang, Y. (2013). Graphene-wrapped CoS nanoparticles for high-capacity lithium-ion storage. ACS applied materials & interfaces, 5(3), 801-806.

[102] Paek, S. M., Yoo, E., & Honma, I. (2008). Enhanced cyclic performance and lithium storage capacity of SnO_2/graphene nanoporous electrodes with three-dimensionally delaminated flexible structure. Nano letters, 9(1), 72-75.

[103] Yue, W., Yang, S., Liu, Y., & Yang, X. (2013). A facile synthesis of mesoporous graphene-tin composites as high-performance anodes for lithium-ion batteries. Materials Research Bulletin, 48(4), 1575-1580.

[104] Xie, G., Zhang, K., Guo, B., Liu, Q., Fang, L., & Gong, J. R. (2013). Graphene Based Materials for Hydrogen Generation from Light Driven Water Splitting. Advanced materials, 25(28), 3820-3839.

[105] Laursen, A. B., Kegnæs, S., Dahl, S., & Chorkendorff, I. (2012). Molybdenum sulfides—efficient and viable materials for electro-and photoelectrocatalytic hydrogen evolution. Energy & Environmental Science, 5(2), 5577-5591.

[106] Liang, Y., Li, Y., Wang, H., & Dai, H. (2013). Strongly coupled inorganic/nanocarbon hybrid materials for advanced electrocatalysis. Journal of the American Chemical Society, 135(6), 2013-2036.

[107] Hinnemann, B., Moses, P. G., Bonde, J., Jørgensen, K. P., Nielsen, J. H., Horch, S., ... & Nørskov, J. K. (2005). Biomimetic hydrogen evolution: MoS2 nanoparticles as catalyst for hydrogen evolution. Journal of the American Chemical Society, 127(15), 5308-5309.

[108] Cobo, S., Heidkamp, J., Jacques, P. A., Fize, J., Fourmond, V., Guetaz, L., ... & Fontecave, M. (2012). A Janus cobalt-based catalytic material for electro-splitting of water. Nature materials, 11(9), 802

[109] Kong, D., Cha, J. J., Wang, H., Lee, H. R., & Cui, Y. (2013). First-row transition metal dichalcogenide catalysts for hydrogen evolution reaction. Energy & Environmental Science, 6(12), 3553-3558.

[110] Li, Y., Wang, H., Xie, L., Liang, Y., Hong, G., & Dai, H. (2011). MoS2 nanoparticles grown on graphene: an advanced catalyst for the hydrogen evolution reaction. Journal of the American Chemical Society, 133(19), 7296-7299.

[111] Zheng, Y., Jiao, Y., Li, L. H., Xing, T., Chen, Y., Jaroniec, M., & Qiao, S. Z. (2014). Toward design of synergistically active carbon-based catalysts for electrocatalytic hydrogen evolution. ACS nano, 8(5), 5290-5296.

[112] Huang, X., Zhao, Y., Ao, Z., & Wang, G. (2014). Micelle-template synthesis of nitrogen-doped mesoporous graphene as an efficient metal-free electrocatalyst for hydrogen production. Scientific reports, 4, 7557.

[113] Liao, L., Zhu, J., Bian, X., Zhu, L., Scanlon, M. D., Girault, H. H., & Liu, B. (2013). MoS2 formed on mesoporous graphene as a highly active catalyst for hydrogen evolution. Advanced Functional Materials, 23(42), 5326-5333.

[114] Li, W., Wu, Z., Wang, J., Elzatahry, A. A., & Zhao, D. (2013). A perspective on mesoporous TiO2 materials. Chemistry of Materials, 26(1), 287-298.

[115] Wan, Y., & Zhao, D. (2007). On the controllable soft-templating approach to mesoporous silicates. Chemical reviews, 107(7), 2821-2860.

[116] Schüth, F. (2001). Non-siliceous mesostructured and mesoporous materials. Chemistry of Materials, 13(10), 3184-3195.

[117] Ren, Y., Ma, Z., & Bruce, P. G. (2012). Ordered mesoporous metal oxides: synthesis and applications. Chemical Society Reviews, 41(14), 4909-4927.

[118] Chen, X., Liu, L., Peter, Y. Y., & Mao, S. S. (2011). Increasing solar absorption for photocatalysis with black hydrogenated titanium dioxide nanocrystals. Science, 331(6018), 746-750.

[119] Livage, J.; Henry, M.; Sanchez, C. Prog. Solid State Chem. 1988, 18, 259.

[120] Yang, H., & Zhao, D. (2005). Synthesis of replica mesostructures by the nanocasting strategy. Journal of Materials Chemistry, 15(12), 1217-1231.

[121] Lu, A. H., & Schüth, F. (2006). Nanocasting: a versatile strategy for creating nanostructured porous materials. Advanced Materials, 18(14), 1793-1805.

[122] Livage, J. A. C. Q. U. E. S., Henry, M., & Sanchez, C. (1988). Sol-gel chemistry of transition metal oxides. Progress in solid state chemistry, 18(4), 259-341.

[123] Kim, D. S., & Kwak, S. Y. (2007). The hydrothermal synthesis of mesoporous TiO2 with high crystallinity, thermal stability, large surface area, and enhanced photocatalytic activity. Applied Catalysis A: General, 323, 110-118.

[124] Sreethawong, T., & Yoshikawa, S. (2005). Comparative investigation on photocatalytic hydrogen evolution over Cu-, Pd-, and Au-loaded mesoporous TiO2 photocatalysts. Catalysis Communications, 6(10), 661-668.

[125] Iijima, S. (1991). Helical microtubules of graphitic carbon. nature, 354(6348), 56.

[126] Schadler, L. S., Giannaris, S. A., & Ajayan, P. M. (1998). Load transfer in carbon nanotube epoxy composites. Applied physics letters, 73(26), 3842-3844.

[127] Ebbesen, T. W., Lezec, H. J., Hiura, H., Bennett, J. W., Ghaemi, H. F., & Thio, T. (1996). Electrical conductivity of individual carbon nanotubes. Nature, 382(6586), 54.

[128] Dillon, A., Jones, K. M., Bekkedahl, T. A., Kiang, C. H., Bethune, D. S., & Heben, M. J. (1997). Storage of hydrogen in single-walled carbon nanotubes. Nature, 386(6623), 377.

[129] Long, R. Q., & Yang, R. T. (2001). Carbon nanotubes as superior sorbent for dioxin removal. Journal of the American Chemical Society, 123(9), 2058-2059.

[130] Li, Y. H., Wang, S., Cao, A., Zhao, D., Zhang, X., Xu, C., ... & Wei, B. (2001). Adsorption of fluoride from water by amorphous alumina supported on carbon nanotubes. Chemical Physics Letters, 350(5-6), 412-416.

[131] Yu, Y., Jimmy, C. Y., Yu, J. G., Kwok, Y. C., Che, Y. K., Zhao, J. C., ... & Wong, P. K. (2005). Enhancement of photocatalytic activity of mesoporous TiO2 by using carbon nanotubes. Applied Catalysis A: General, 289(2), 186-196.

[132] Keith, L., & Telliard, W. (1979). ES&T special report: priority pollutants: Ia perspective view. Environmental science & technology, 13(4), 416-423.

[133] Janda, V., & Svecova, M. (1997). By-products in drinking water disinfection. Feedback, 91.

[134] Yue, B., Zhou, Y., Xu, J., Wu, Z., Zhang, X., Zou, Y., & Jin, S. (2002). Photocatalytic degradation of aqueous 4-chlorophenol by silica-immobilized polyoxometalates. Environmental science & technology, 36(6), 1325-1329.

[135] Mantilla, A., Jácome-Acatitla, G., Morales-Mendoza, G., Tzompantzi, F., & Gómez, R. (2010). Photoassisted degradation of 4-chlorophenol and p-cresol using MgAl hydrotalcites. Industrial & Engineering Chemistry Research, 50(5), 2762-2767.

[136] Rathouskı, J., Kalousek, V., Koláø, M., & Jirkovskı, J. (2011). Mesoporous films of TiO 2 as efficient photocatalysts for the purification of water. Photochemical & Photobiological Sciences, 10(3), 419-424.

[137] Abida, O., Kolar, M., Jirkovsky, J., & Mailhot, G. (2012). Degradation of 4-chlorophenol in aqueous solution photoinduced by Fe (III)–citrate complex. Photochemical & Photobiological Sciences, 11(5), 794-802.

[138] Zhou, M., Yu, J., & Cheng, B. (2006). Effects of Fe-doping on the photocatalytic activity of mesoporous TiO2 powders prepared by an ultrasonic method. Journal of Hazardous Materials, 137(3), 1838-1847.

[139] Yang, P., Gai, S., & Lin, J. (2012). Functionalized mesoporous silica materials for controlled drug delivery. Chemical Society Reviews, 41(9), 3679-3698.

[140] Huh, S., Wiench, J. W., Yoo, J. C., Pruski, M., & Lin, V. S. Y. (2003). Organic functionalization and morphology control of mesoporous silicas via a co-condensation synthesis method. Chemistry of materials, 15(22), 4247-4256.

[141] Trewyn, B. G., Whitman, C. M., & Lin, V. S. Y. (2004). Morphological control of room-temperature ionic liquid templated mesoporous silica nanoparticles for controlled release of antibacterial agents. Nano Letters, 4(11), 2139-2143.

[142] Suzuki, K., Ikari, K., & Imai, H. (2004). Synthesis of silica nanoparticles having a well-ordered mesostructure using a double surfactant system. Journal of the American Chemical Society, 126(2), 462-463.

[143] Gilroy, K. D. (2015). Shape-engineering substrate-based plasmonic nanomaterials. Temple University.

[144] Ying, J. Y., Mehnert, C. P., & Wong, M. S. (1999). Synthesis and applications of supramolecular templated mesoporous materials. Angewandte Chemie International Edition, 38(1 2), 56-77.

[145] Kresge, C. T., Leonowicz, M. E., Roth, W. J., Vartuli, J. C., & Beck, J. S. (1992). Ordered mesoporous molecular sieves synthesized by a liquid-crystal template mechanism. nature, 359(6397), 710.

[146] Radu, D. R., Lai, C. Y., Jeftinija, K., Rowe, E. W., Jeftinija, S., & Lin, V. S. Y. (2004). A polyamidoamine dendrimer-capped mesoporous silica nanosphere-based gene transfection reagent. Journal of the American Chemical Society, 126(41), 13216-13217.

[147] Slowing, I., Trewyn, B. G., & Lin, V. S. Y. (2006). Effect of surface functionalization of MCM-41-type mesoporous silica nanoparticles on the endocytosis by human cancer cells. Journal of the American Chemical Society, 128(46), 14792-14793

[148] Wan, Y., & Zhao, D. (2007). On the controllable soft-templating approach to mesoporous silicates. Chemical reviews, 107(7), 2821-2860.

[149] Monnier, A., F. Schuth, Q. Kumar, D. Margolese, R. MAXWELL, G. D. Stuky, M. Krisnamurthy et al. "High-Resolution Transmission Electron Micros-copy of Mesoporous MCM-41 Type Materials." (1993): 1299-1299.

[150] Zhao, D., Sun, J., Li, Q., & Stucky, G. D. (2000). Morphological control of highly ordered mesoporous silica SBA-15. Chemistry of Materials, 12(2), 275-279.

[151] Huo, Q., Margolese, D. I., & Stucky, G. D. (1996). Surfactant control of phases in the synthesis of mesoporous silica-based materials. Chemistry of Materials, 8(5), 1147-1160.

[152] Huo, Q., Feng, J., Schüth, F., & Stucky, G. D. (1997). Preparation of hard mesoporous silica spheres. Chemistry of Materials, 9(1), 14-17.

[153] Schacht, S., Huo, Q., Voigt-Martin, I. G., Stucky, G. D., & Schüth, F. (1996). Oil-water interface templating of mesoporous macroscale structures. Science, 273(5276), 768-771.

[154] Ozin, G. (1998). Synthesis of mesoporous silica spheres under quiescent aqueous acidic conditions. Journal of Materials Chemistry, 8(3), 743-750.

[155] Lu, Y., Fan, H., Stump, A., Ward, T. L., Rieker, T., & Brinker, C. J. (1999). Aerosol-assisted self-assembly of mesostructured spherical nanoparticles. Nature, 398(6724), 223.

[156] Nakamura, R., & Frei, H. (2006). Visible light-driven water oxidation by Ir oxide clusters coupled to single Cr centers in mesoporous silica. Journal of the American Chemical Society, 128(33), 10668-10669.

[157] De Vos, D. E., Dams, M., Sels, B. F., & Jacobs, P. A. (2002). Ordered mesoporous and microporous molecular sieves functionalized with transition metal complexes as catalysts for selective organic transformations. Chemical Reviews, 102(10), 3615-3640.

[158] Hoertz, P. G., & Mallouk, T. E. (2005). Light-to-chemical energy conversion in lamellar solids and thin films. Inorganic chemistry, 44(20), 6828-6840.

[159] Das, S. K., & Dutta, P. K. (1998). Synthesis and characterization of a ruthenium oxide–zeolite Y catalyst for photochemical oxidation of water to dioxygen1. Microporous and mesoporous materials, 22(1-3), 475-483.

[160] Hammarström, L. (2003). Towards artificial photosynthesis: ruthenium–manganese chemistry mimicking photosystem II reactions. Current opinion in chemical biology, 7(6), 666-673.

[161] Lin, W., & Frei, H. (2005). Photochemical CO2 splitting by metal-to-metal charge-transfer excitation in mesoporous ZrCu (I)-MCM-41 silicate sieve. Journal of the American Chemical Society, 127(6), 1610-1611.

[162] Kuwahara, Y., & Yamashita, H. (2011). Efficient photocatalytic degradation of organics diluted in water and air using TiO 2 designed with zeolites and mesoporous silica materials. Journal of Materials Chemistry, 21(8), 2407-2416.

[163] Tanaka, D., Oaki, Y., & Imai, H. (2010). Enhanced photocatalytic activity of quantum-confined tungsten trioxide nanoparticles in mesoporous silica. Chemical Communications, 46(29), 5286-5288.

[164] Hotchandani, S., Bedja, I., Fessenden, R., & Kamat, P. (1994). Electrochromic and Photoelectrochromic Behavior of Thin WO3 Films Prepared from Quantum Size Collodal Particles. Langmuir, 10(1), 17-22.

[165] Balázsi, C., Wang, L., Zayim, E. O., Szilágyi, I. M., Sedlacková, K., Pfeifer, J., ... & Gouma, P. I. (2008). Nanosize hexagonal tungsten oxide for gas sensing applications. Journal of the European Ceramic Society, 28(5), 913-917.

[166] Zhou, J., Gong, L., Deng, S. Z., Chen, J., She, J. C., Xu, N. S., ... & Wang, Z. L. (2005). Growth and field-emission property of tungsten oxide nanotip arrays. Applied Physics Letters, 87(22), 223108.

[167] Abe, R., Takami, H., Murakami, N., & Ohtani, B. (2008). Pristine simple oxides as visible light driven photocatalysts: highly efficient decomposition of organic compounds over platinum-loaded tungsten oxide. Journal of the American Chemical Society, 130(25), 7780-7781.

[168] Le Houx, N., Pourroy, G., Camerel, F., Comet, M., & Spitzer, D. (2009). WO3 nanoparticles in the 5" 30 nm range by solvothermal synthesis under microwave or resistive heating. The Journal of Physical Chemistry C, 114(1), 155-161.

[169] Chiang, T. H., Hsu, C. C., Chen, T. M., & Yu, B. S. (2015). Synthesis and structural characterization of tungsten oxide particles by the glycothermal method. Journal of Alloys and Compounds, 648, 297-306.

[170] Lu, Z., Kanan, S. M., & Tripp, C. P. (2002). Synthesis of high surface area monoclinic WO 3 particles using organic ligands and emulsion-based methods. Journal of Materials Chemistry, 12(4), 983-989.

[171] Brus, L. (1986). Electronic wave functions in semiconductor clusters: experiment and theory. The Journal of Physical Chemistry, 90(12), 2555-2560.

[172] Vossmeyer, T., Katsikas, L., Giersig, M., Popovic, I. G., Diesner, K., Chemseddine, A., ... & Weller, H. (1994). CdS nanoclusters: synthesis, characterization, size dependent oscillator strength, temperature shift of the excitonic transition energy, and reversible absorbance shift. The Journal of Physical Chemistry, 98(31), 7665-7673.

[173] Colvin, V. L., Schlamp, M. C., & Alivisatos, A. P. (1994). Light-emitting diodes made from cadmium selenide nanocrystals and a semiconducting polymer. Nature, 370(6488), 354.

[174] Zhu, K., Shi, J., & Zhang, L. (1998). Preparation and optical absorption of InSb microcrystallites embedded in SiO2 thin films. Solid state communications, 107(2), 79-84.

[175] Liu, Z., Zhao, Z. G., & Miyauchi, M. (2009). Efficient visible light active CaFe2O4/WO3 based composite photocatalysts: effect of interfacial modification. The Journal of Physical Chemistry C, 113(39), 17132-17137.

[176] Tauc, J., Grigorovici, R., & Vancu, A. (1966). Optical properties and electronic structure of amorphous germanium. physica status solidi (b), 15(2), 627-637.

[177] Arai, T., Horiguchi, M., Yanagida, M., Gunji, T., Sugihara, H., & Sayama, K. (2008). Complete oxidation of acetaldehyde and toluene over a Pd/WO 3 photocatalyst under fluorescent-or visible-light irradiation. Chemical Communications, (43), 5565-5567.

[178] Huang, C. H., Chang, K. P., Ou, H. D., Chiang, Y. C., Chang, E. E., & Wang, C. F. (2011). Characterization and application of Ti-containing mesoporous silica for dye removal with synergistic effect of coupled adsorption and photocatalytic oxidation. Journal of hazardous materials, 186(2-3), 1174-1182.